CSIRO PUBLISHING
www.publish.csiro.au/journals/is *Invertebrate Systematics*, 2005, **19**, 145–168

The evolutionary relationships of North American *Diplous* Motschulsky (Coleoptera : Carabidae : Patrobini) inferred from morphological and molecular evidence

Paul E. Marek[A,B,C,D] *and David H. Kavanaugh*[A]

[A]Department of Entomology, California Academy of Sciences, Golden Gate Park, San Francisco, California 94118, USA.
[B]Department of Biology, San Francisco State University, 1600 Holloway Avenue, San Francisco, California 94132, USA.
[C]Current address: Department of Biology, East Carolina University, Howell Science Complex, Greenville, North Carolina 27858, USA.
[D]Corresponding author. Email: pm0623@mail.ecu.edu

Abstract. Individuals of the ground beetle genus *Diplous* Motschulsky, 1850 occur in riparian areas predominately throughout boreal North America and Asia. In order to infer the species phylogeny of the North American *Diplous*, we examined 97 morphological characters (56 quantitative characters and 41 qualitative characters) and 458 bp of the mitochondrial cytochrome oxidase subunit I region. We used the four North American species, four Palearctic species, and one undescribed species of a closely related genus to test the monophyly and the direction of character state change in North American *Diplous*. Overall, we found that North American *Diplous* appear to represent a monophyletic group, but that the morphological and molecular evidence did not support the same relationships in the placement of one of the species. We found that the total evidence trees agreed most with biogeography and considerations of accelerated morphological evolution. In this paper, we present a morphological phylogenetic tree, a molecular phylogenetic tree, a total evidence phylogenetic tree, a species key, species diagnoses, and a distribution map of Nearctic *Diplous*.

Additional keywords: *COI*, cytochrome oxidase subunit I, *Diplous*, glacier, ground beetle, *Platidius*, Pleistocene, refugia, riparian, total evidence, vicariance.

Introduction

The beetle family Carabidae Latreille, 1810 comprises ~30 000 (Reichardt 1977) to 40 000 (Erwin 1991) known species that occur in a diversity of habitats from between 78.93°N latitude and 55.00°S latitude and from sea-level to above 5000 m in the Himalayas (Ball and Bousquet 2001).

Members of the genus *Diplous* Motschulsky, 1850 are riparian ground beetles associated with rocky, gravelly stream banks in North America and Asia between 25.28°N latitude (Gaoligong Mountains in south-western China) and 68.85°N latitude (Bayas River in Russia), to 63.30°W longitude (Truro in Nova Scotia) and 83.51°E longitude (Leninogorsk in Kazakhstan), and between sea-level (Chicagof I. in Alaska) to 4850 m (Rongpu Si in Tibet). *Diplous* occur in the lacunae between and under rocks and eat smaller invertebrates. Presumably to fit in these cracks and crevices, members of this genus have a more dorsoventrally flattened body than other related ground beetles, like *Patrobus* Chaudoir, 1871 species. *Diplous* species can be distinguished from those of *Patrobus* by their depressed shape and the following characters (that are probably linked to this flattening): shallow occipital constriction, shallow median longitudinal impression, and broadly triangular mesepimeron (Darlington 1938). The centre of diversity for this group is western China (predominately in the Sichuan Province) and Tibet. The genus is placed in the Holarctic tribe Patrobini, which comprises ~180 species in 15 genera, of which 12 species and four genera occur in the Nearctic subregion. Patrobine ground beetles can be diagnosed by the presence of a ring sclerite on the dorsal surface of the bursal sac in females. Though it is unclear whether this character is a tribal synapomorphy, it is a useful diagnostic character because it consistently appears in all female patrobines. Maddison *et al*. (1999) demonstrated the monophyly of the supertribe Trechitae including Patrobini, in a phylogeny of ground beetles based on 18s rDNA sequence data and previous cytogenetic and morphological evidence.

Taxonomic history

The genus *Diplous* was first described in 1850 by Motschulsky, based on the Palearctic species *Patrobus*

© CSIRO 2005
10.1071/IS04011 1445-5226/05/020145

sibiricus Motschulsky, 1844. In 1871, Chaudoir established the genus *Platidius* based on the deeply bifid emargination of the fourth tarsal segment of the Nearctic species, *Diplous aterrimus* (Dejean, 1828), asserting its distinction from the *Diplous* species of the Palearctic. Shortly after, Bates (1873), in his description of the Palearctic species *Diplous caligatus*, synonymised *Platidius* with *Diplous*. He maintained that the characteristics used by Chaudoir were insignificant for a generic-level distinction. Although Bates suggested this synonymy, his writing was somewhat indecisive and note-like; therefore his synonymy was not upheld. In his excellent revision of the tribe Patrobini, Darlington (1938) followed Chaudoir by formally designating *Platidius aterrimus* as type species for the genus. This was a tentative, though formal, decision and he 'prefer[red] to follow Chaudoir until the synonymy [could] be settled more definitely' (Darlington 1938: 147). Kühnelt (1941) suggested junior synonymy for *Platidius*. Like Bates (1873), he maintained that the characters were not sufficient for a genus, but instead supported a Nearctic subgenus, *Platidius*. In 1961: 186, Lindroth accepted Kühnelt's opinion and agreed that the distinguishing characters used by Chaudoir (1871) 'are not very important'. Lindroth also agreed that 'all North American species belong to the subgenus *Platidius*', as designated by Kühnelt (1941), using characters of the aedeagus.

In 1941, Kühnelt published a monograph on the genus *Diplous*. In this work, using no formal criteria, he apportioned the species into three species groups: Group 1, containing *D. caligatus* Bates, 1873 and *D. sibiricus*; Group 2, containing *D. depressus* (Gebler, 1829) and *D. przewalskii* Semenow, 1889; and Group 3, containing *D. californicus* (Motschulsky, 1859), *D. aterrimus*, *D. filicornis* (Casey, 1918), and *D. rugicollis* (Randall, 1838). To date, 22 Holarctic species of *Diplous* have been described. Four species occur in the Nearctic subregion and eighteen exist in the Palearctic subregion. The species are divided into five species groups:

aterrimus-group

- *D. californicus* (Motschulsky, 1859)
- *D. aterrimus* (Dejean, 1828)
- *D. filicornis* (Casey, 1918)
- *D. rugicollis* (Randall, 1838)
- *D. depressus* (Gebler, 1829)

sibiricus-group

- *D. sibiricus sibiricus* (Motschulsky, 1844)
- *D. sibiricus caligatus* Bates, 1873
- *D. sibiricus atratus* Habu, 1951
- *D. sibiricus yezoensis* Habu, 1941
- *D. sterbai* Jedlička, 1932
- *D. gansuensis* Jedlička, 1932
- *D. yunnanus* Jedlička, 1932
- *D. szetchuanus* Jedlička, 1932

przewalskii-group

- *D. przewalskii* Semenow, 1889
- *D. grummi grummi* Zamotajlov & Kryzhanovskij, 1990
- *D. grummi bicolor* Zamotajlov & Sciaky, 1996
- *D. tonggulensis* Zamotajlov & Sciaky, 1996
- *D. sciakyi sciakyi* Zamotajlov, 1996
- *D. sciakyi fedorenkoi* Zamotajlov, 1996
- *D. sciakyi grandis* Zamotajlov, 1996
- *D. wrasei* Zamotajlov, 1996
- *D. petrogorbatschevi* Zamotajlov, 1996
- *D. wulanensis* Zamotajlov, 1997

davidis-group

- *D. davidis* (Fairmaire, 1891)
- *D. nortoni* Andrews, 1930
- *D. jedlickai* Zamotajlov, 1996
- *D. julonshanensis* Zamotajlov, 1993

giacomazzoi-group

- *D. giacomazzoi* Zamotajlov & Sciaky, 1996

To date, only pairwise comparisons of morphology have been used to explain species relationships; most of these hypotheses have been based on overall similarity without any reference to phylogeny.

In this study, we attempt to clarify the species relationships and test the monophyly of the North American *Diplous* species. By using different datasets and various phylogenetic methods, we hoped to obtain a well corroborated and robust phylogeny. We also describe biogeographical patterns, summarise the taxonomy, and provide diagnoses and a key to North American *Diplous*.

Materials and methods

Materials

A total of 595 specimens were examined in the course of this study. Material was obtained on loan from the following institutions:

BMNH	The Natural History Museum, London, England
CASC	California Academy of Sciences, San Francisco, California, USA
IOZB	Institute of Zoology, Chinese Academy of Sciences, Beijing, China

Type material referred to below is deposited in the following institutions:

MCZ	Museum of Comparative Zoology at Harvard University, Cambridge, Massachussetts, USA
MNHN	Muséum National d'Histoire Naturelle, Paris, France
USNM	National Museum of Natural History, Smithsonian Institution, Washington, USA
ZMMU	Zoological Museum, Moscow State University, Moscow, Russia

Full details of material examined are available on the *Invertebrate Systematics* website in Accessory Publication – MatEx.

Taxon sampling

For the morphological dataset, we used both males and females of five ingroup taxa (i.e. the four North American species and the Palearctic species, *D. depressus*) and the outgroup taxa, *D. sibiricus caligatus*, *D. sciakyi sciakyi*, *D. davidis*, and a species of *Qiangopatrobus* Zamotajlov 2002. For the molecular, *COI* dataset, we used 12 ingroup sequences spanning the four North American species and two outgroup sequences from a species of a closely related Palearctic genus, *Qiangopatrobus* (Table 1).

Dissections

We dissected male and female genitalia of all the ingroup and outgroup taxa. Pinned and dried specimens were softened in hot water and detergent for 30 min. After a beetle was sufficiently softened, we extracted the female bursa copulatrix and the male aedeagus and all structures associated with them. The dissected parts were then cleared in a 10% KOH (Fisher Scientific Co., Hampton, NH, USA) solution. Females remained in the solution for ten minutes and males for five minutes. We then put the parts into water to dilute the KOH. The endophallus of the aedeagus was usually retracted into the median lobe. We pushed out the endophallus with a small pipette tip and a syringe in order to see features of the apical accessory piece and endophallic sac. After the dissected parts were no longer reacting with KOH, we stained them with chlorazol black E (Fisher Scientific Co.). Once stained, the preparations were examined and photographed. Ultimately, the dissected parts were stored in microvials containing glycerin and pinned beneath their specimen of origin and its labels.

We assessed 97 morphological characters, which included both quantitative (morphometric) and qualitative characters (Table 2). We measured 33 anatomical features of the exoskeleton in males and 27 in females using a Leica 9.5 stereomicroscope (Leica Microsystems AG, Wetzler, Germany) equipped with an eyepiece graticule. In order to measure each part, we placed the specimen so that the ends of the structure to be measured were in a plane perpendicular to the line of sight and parallel to the eyepiece graticule. After we measured specimens, we made Q-Q probability plots in SPSS ver. 11.5 (SPSS Inc., Chicago, IL, USA) to determine if the within species measurement distributions matched a normal distribution and to check if a transformation was necessary. Of the 60 measurement distributions in both males and females, 42 were consistent with a normal distribution. Of the set of measurement distributions, 18 were not consistent with a normal distribution. Each of these characters contained one extreme datapoint (i.e. those cases with values more than 3 interquartile ranges greater or less than the 1st and 3rd quartile value) that was so divergent from the distribution of the other values that they precluded determining the nature of the distribution in a Q-Q probability plot. We excluded those extreme datapoints. We believe that these wildly divergent values were a result of measurement errors or highly aberrant specimens and therefore justifiably omitted from the specimen sample. Subsequently, all 60 measurement distributions matched a normal distribution. We also included a set of 41 qualitative characters in our phylogenetic analysis. First, we imaged the head (dorsum), pronotum (dorsum), elytra (dorsum), head and pronotum (lateral), and abdomen (venter) of the specimens using a CoolPix® 995 digital camera (Nikon Co., Tokyo, Japan) mounted on a Leica 9.5 stereomicroscope; second, we developed hypotheses of character state homology by comparing these images of the body regions; and third we coded 41 qualitative, multistate characters based on these hypotheses. Illustrations of character states are available for download on the *Invertebrate Systematics* website in Accessory Publication – Characters.

DNA amplification and sequencing

We used thoracic wing muscle tissue cut from fresh specimens killed and preserved in 95% ethyl alcohol. The wing muscles are large and easily removed. Exclusive use of wing muscles avoids any foreign DNA associated with gut parasites. Conveniently, the beetle specimen is only slightly damaged in this process, leaving most of the specimen to be pinned and designated as a voucher specimen.

We sequenced a portion of one mitochondrial gene: a 458 base pair region of *COI* amplified by the primer pair C1-J-1751-5′ and C1-N-2191-3′ (Simon *et al*. 1994). This region is a part of cytochrome oxidase that is the last enzyme in the electron transport chain. It is responsible for reducing oxygen to water and pumping a proton across the membrane in order to contribute to the proton gradient driving ATP synthesis.

We amplified the *COI* region using the following PCR steps, an initial denaturing step, a secondary denaturing step, an annealing step, and an extension step: *1*. 94.0°C for 1:30 min; *2*. 94.0°C for 0:30 min; *3*. 56.0°C for 0:45 min; *4*. 72.0°C for 0:45 min; *5*. GOTO 2, 29×. We cleaned the amplified DNA using Qiagen Qiaquick® (Valencia, CA) spin tubes to remove any remaining unincorporated base pairs or extraneous products left over from amplification, and sequenced them using an ABI 377 sequencing machine. The sequences were easily aligned in Sequencher 3.1.1 (Gene Codes Co., Ann Arbor, MI, USA) and then exported to PAUP* ver. 4.0b10 (Swofford 2002). All voucher specimens for the molecular analysis were deposited at CASC.

Phylogenetic analysis of morphological data

We included all four North American species of *Diplous* and the Palearctic species *Diplous depressus* as ingroup terminals (see Accessory Publication – Specimens (morphology) on the *Invertebrate Systematics* website). We used three Palearctic species, *Diplous sibiricus caligatus*, *Diplous davidis*, *Diplous sciakyi sciakyi*, and one species of a closely related genus of ground beetle in the same tribe as *Diplous* to root the ingroup taxa (Watrous and Wheeler 1981). This species belongs to the Palearctic genus *Qiangopatrobus*, which is hypothesised to be the sister-group of the Holarctic species of *Diplous* (Zamotajlov 2002).

We used step-matrix gap weighting (Wiens 2001), a modification of gap weighting of Thiele (1993), to code continuous characters in our phylogenetic analysis. Step-matrix gap weighting operates on the principal that a character state is a frequency distribution of potentially overlapping attributes (in our case ratios derived from morphometries) in a sample of individuals in a taxon (Thiele 1993). This frequency distribution of attributes, as a character in the cladistic sense, which logically cannot overlap, is expressed as a median value (or mean value, depending on the nature of the distribution). This median value, after range standardisation, operates as a character state. Each species has a different attribute distribution, a different median value, and therefore a different character state (hence the number of character states equals the number of species). The character state difference, the difference between two median ratio values, acts to quantify the evolutionary cost of transitioning from one character state to another in a phylogenetic analysis under parsimony by inputting the cost value into a step-matrix. From the 60 quantitative morphometries (Figs 1, 2), we calculated a set of 56 ratios for both males and females (Appendix 1). We used these ratios to quantify differences in the shapes and relative proportions of the structures. These ratios consistently deviated from a normal distribution when plotted against expected values in a Q-Q probability scatterplot. Because the ratios in a given species were not normally distributed, we chose to not use the mean as a measure of central tendency. Instead, we used the median ratio value (x) to calculate a standardised value (x_s) according to the equation:

$$x_s = (x - \min)/(\max - \min) \times 999$$

In this equation ‘min’ is the minimum median ratio value across all the species and ‘max’ the maximum median ratio value across all the species. The value ‘999’ is the maximum cost for state transistions in MacClade 4.0 (Maddison and Maddison 2000); such a large value allows for precise standardisation of a range of character ratio median

Table 1. DNA specimen localities
Elev., elevation

Species	NCBI Acc.	Specimen	Country	State	County	Label	Latitude °N	Longitude °W	Elev. (m)	Date	Collector
Diplous aterrimus	DQ058775	7	USA	Washington		Hoh Rainforest				22.iii.2001	T.Mastranicola
D. aterrimus	DQ058772	8	USA	Washington		Hoh Rainforest				22.iii.2001	T.Mastranicola
D. californicus	DQ058776	1	USA	California	Humboldt	Humboldt State Redwood Park	40.3709	–123.9192	52	12.iv.2001	P.Marek
D. californicus	DQ058778	2	USA	California	Trinity	Skunk Group Campground	40.7330	–123.2290		11.iv.2001	P.Marek
D. filicornis	DQ058767	12	USA	California	Sierra	Wild Plum Campground	39.5660	–120.5980	427	10.vii.2001	P.Marek
D. filicornis	DQ058770	5	USA	California	Mendocino	Jackson State Forest			61	13.iv.2001	P.Marek
D. filicornis	DQ058773	6	USA	California	Mendocino	Jackson State Forest			61	13.iv.2001	P.Marek
D. filicornis	DQ058768	3	USA	California	Siskiyou	Ney Springs Creek	41.2670	–122.3120	305	10.iv.2001	P.Marek
D. filicornis	DQ058769	4	USA	California	Siskiyou	Ney Springs Creek	41.2670	–122.3120	305	10.iv.2001	P.Marek
D. rugicollis	DQ058774	11	USA	Maine	Franklin	Sandy River	44.8533	–70.4350	174	12.vii.2001	R.E.Nelson
D. rugicollis	DQ058771	9	USA	Maine	Somerset	Austin Stream	45.0650	–69.8817	113	14.vii.2001	R.E.Nelson
D. rugicollis	DQ058777	10	USA	Maine	Somerset	Austin Stream	45.0650	–69.8817	113	14.vii.2001	R.E.Nelson
Qiangopatrobus sp.	DQ058765	14	China	Yunnan	Nujiang	Gaoligongshan, No. 12 Br. Camp	27.7150	98.5024	2775	15–19.vii.2000	D.H.Kavanaugh
Qiangopatrobus sp.	DQ058766	13	China	Yunnan	Nujiang	Gaoligongshan, Qiqi He	27.7154	98.5653	2000	14.vii.2000	D.H.Kavanaugh

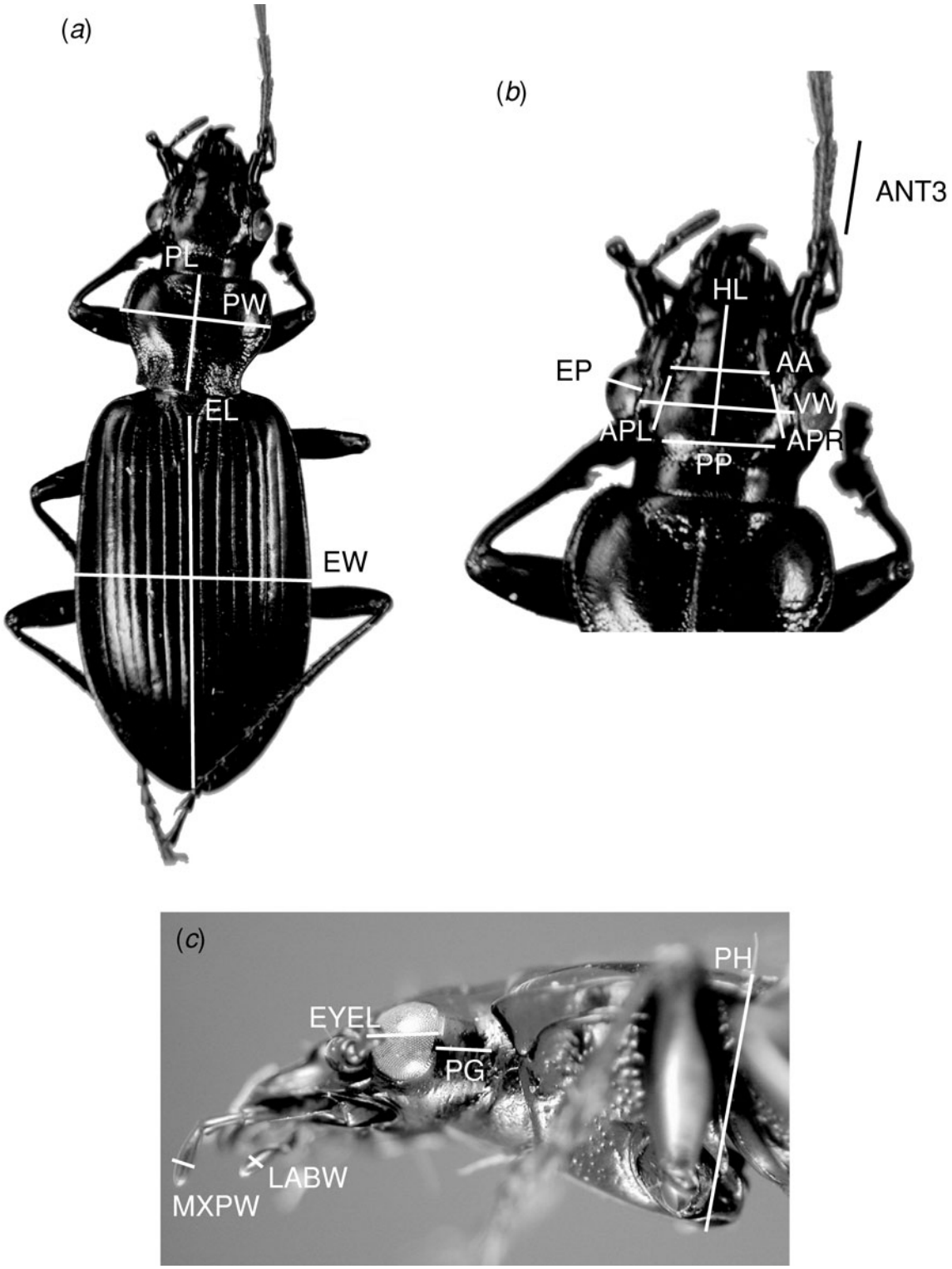

Fig. 1. Morphometries from which ratios were calculated. (*a*) Measurements of the pronotum and elytra, dorsal view (PL, pronotum length; PW, pronotum width; EL, elytral length; EW, elytral width). (*b*) Measurements of the head, dorsal view (ANT3, left third antennomere length; HL, head length; EP, left eye protuburance; APL, length between left anterior supraorbital seta to left posterior supraorbital seta; PP, length between left posterior supraorbital seta to right posterior supraorbital seta; APL, length between left anterior supraorbital seta to left posterior supraorbital seta; VW, vertex width; AA, length between left anterior supraorbital seta to right anterior supraorbital seta). (*c*) Measurements of the head and pronotum, lateral view (MXPW, left maxillary palpomere 3 width; LABW, left labial palpomere 3 width; EYEL, left eye length; PG, left postgenae length; PH, pronotum height).

Table 2. Characters used in the analysis

Quantitative: morphometric ratios

(*1*) ♂ *MXPW/VW*: left maxillary palpomere 3 width / vertex width (*CI* = 0.600)
(*2*) ♂ *LABW/MXPW*: left labial palpomere 3 width / left maxillary palpomere 3 width (*CI* = 0.588)
(*3*) ♂ *ANT3/HL*: left third antennomere length / head length (*CI* = 0.494)
(*4*) ♂ *HL/PL*: head length / pronotum length (*CI* = 0.674)
(*5*) ♂ *EP/VW*: left eye protuburance / vertex width (*CI* = 0.682)
(*6*) ♂ *VW/PW*: vertex width / pronotum width (*CI* = 0.647)
(*7*) ♂ *EYEL/HL*: left eye length / head length (*CI* = 0.539)
(*8*) ♂ *PG/HL*: left postgenae length / head length (*CI* = 0.806)
(*9*) ♂ *APL/HL*: length between left anterior supraorbital seta to left posterior supraorbital seta / head length (*CI* = 0.491)
(*10*) ♂ *APR/HL*: length between right anterior supraorbital seta to right posterior supraorbital seta / head length (*CI* = 0.500)
(*11*) ♂ *AA/VW*: length between left anterior supraorbital seta to right anterior supraorbital seta / vertex width (*CI* = 0.422)
(*12*) ♂ *PP/VW*: length between left posterior supraorbital seta to right posterior supraorbital seta / vertex width (*CI* = 0.645)
(*13*) ♂ *PL/EL*: pronotum length (midline) / elytral length (*CI* = 0.737)
(*14*) ♂ *PW/EW*: pronotum width / elytral width (*CI* = 0.768)
(*15*) ♂ *PH/PL*: pronotum height / pronotum length (midline) (*CI* = 0.533)
(*16*) ♂ *EL/EW*: elytral length / elytral width (*CI* = 0.571)
(17) ♂ *MTTL/MTFL*: left metatrochanter length / left metafemur length (*CI* = 0.792)
(*18*) ♂ *MTFL/EW*: left metafemur length / elytra width (*CI* = 0.474)
(*19*) ♂ *T1/T2*: left protarsomere 1 width / left protarsomere 2 width (*CI* = 0.588)
(*20*) ♂ *T2/T3*: left protarsomere 2 width / left protarsomere 3 width (*CI* = 0.809)
(*21*) ♂ *T3/T4*: left protarsomere 3 width / left protarsomere 4 width (*CI* = 0.601)
(*22*) ♂ *T4/T4L*: left protarsomere 4 width / left protarsomere 4 length (*CI* = 0.705)
(*23*) ♂ *T5/T4*: left protarsomere 5 width / left protarsomere 4 width (*CI* = 0.857)
(*24*) ♂ *T4E/T4L*: left protarsomere 4 emargination / left protarsomere 4 length (*CI* = 0.675)
(*25*) ♂ *AEL/EL*: male aedeagal length / elytral length (*CI* = 0.393)
(*26*) ♂ *AEBL/AEL*: male aedeagal base length / aedeagal length (*CI* = 0.551)
(*27*) ♂ *DCPL/AEL*: male distal copulatory piece length / aedeagal length (*CI* = 0.558)
(*28*) ♂ *LPL/AEL*: male left paramere length / aedeagal length (*CI* = 0.484)
(*29*) ♂ *RPL/AEL*: male right paramere length / aedeagal length (*CI* = 0.589)
(*30*) ♂ *RSL/AEL*: male ring sclerite length / aedeagal length (*CI* = 0.537)
(*31*) ♂ *RSW/RSL*: male ring sclerite width / ring sclerite length (*CI* = 0.652)
(*32*) ♀ *MXPW/VW*: left maxillary palpomere 3 width / vertex width (*CI* = 0.861)
(*33*) ♀ *LABW/MXPW*: left labial palpomere 3 width / left maxillary palpomere 3 width (*CI* = 0.770)
(*34*) ♀ *ANT3/HL*: left third antennomere length / head length (*CI* = 0.630)
(*35*) ♀ *HL/PL*: head length / pronotum length (*CI* = 0.727)
(*36*) ♀ *EP/VW*: left eye protuburance / vertex width (*CI* = 0.521)
(*37*) ♀ *VW/PW*: vertex width / pronotum width (*CI* = 0.658)
(*38*) ♀ *EYEL/HL*: left eye length / head length (*CI* = 0.667)
(*39*) ♀ *PG/HL*: left postgenae length / head length (*CI* = 0.792)
(*40*) ♀ *APL/HL*: length between left anterior supraorbital seta to left posterior supraorbital seta / head length (*CI* = 0.411)
(*41*) ♀ *APR/HL*: length between right anterior supraorbital seta to right posterior supraorbital seta / head length (*CI* = 0.414)
(*42*) ♀ *AA/VW*: length between left anterior supraorbital seta to right anterior supraorbital seta / vertex width (*CI* = 0.489)
(*43*) ♀ *PP/VW*: length between left posterior supraorbital seta to right posterior supraorbital seta / vertex width (*CI* = 0.730)
(*44*) ♀ *PL/EL*: pronotum length (midline) / elytral length (*CI* = 0.787)
(*45*) ♀ *PW/EW*: pronotum width / elytral width (*CI* = 1.000)
(*46*) ♀ *PH/PL*: pronotum height / pronotum length (midline) (*CI* = 0.717)
(*47*) ♀ *EL/EW*: elytral length / elytral width (*CI* = 0.634)
(*48*) ♀ *MTTL/MTFL*: left metatrochanter length / left metafemur length (*CI* = 0.524)
(*49*) ♀ *MTFL/EW*: left metafemur length / elytra width (*CI* = 0.630)
(*50*) ♀ *T1/T2*: left protarsomere 1 width / left protarsomere 2 width (*CI* = 0.861)
(*51*) ♀ *T2/T3*: left protarsomere 2 width / left protarsomere 3 width (*CI* = 0.529)
(*52*) ♀ *T3/T4*: left protarsomere 3 width / left protarsomere 4 width (*CI* = 0.966)
(*53*) ♀ *T4/T4L*: left protarsomere 4 width / left protarsomere 4 length (*CI* = 0.432)
(*54*) ♀ *T5/T4*: left protarsomere 5 width / left protarsomere 4 width (*CI* = 0.604)
(*55*) ♀ *T4E/T4L*: left protarsomere 4 emargination / left protarsomere 4 length (*CI* = 0.989)
(*56*) ♀ *BR/EL*: female bursal ring width / elytral length (*CI* = 0.505)

Qualitative: fixed, multistate (character states are shown in parentheses; illustrations available on the *Invertebrate Systematics* website in Accessory Publication – Characters)

(*57*) ♂ ♀ *Postgenal curvature*: straight (0); convex (1) (*CI* = 0.500) Accessory Publication – Characters/Character57.pdf
(*58*) ♂ ♀ *Mandible color*: black with heavy red tint (0); black with light red tint (1); red with black tint (2) (*CI* = 1.000) Accessory Publication – Characters/Character58.pdf
(*59*) ♂ ♀ *Neck constriction*: lightly impressed (0); moderately impressed (1); deeply impressed (2); very deeply impressed (3) (*CI* = 1.000) Accessory Publication – Characters/Character59.pdf

(*continued next page*)

Table 2. (continued)

(*60*) ♂ ♀ *Neck constriction macrosculpture*: smooth (0); sparsely covered with small punctures dorsomedially (1); sparsely covered with medium-sized punctures dorsomedially (2); sparsely covered with heavy punctures around the dorsal part of the neck (3) (*CI* = 0.600) Accessory Publication – Characters/Character60.pdf
(*61*) ♂ ♀ *Frontal furrow divergence*: 15° (0); 23° (1); 30° (2) (*CI* = 0.400) Accessory Publication – Characters/Character61.pdf
(*62*) ♂ ♀ *Frontal furrow macrosculpture*: impunctate (0); punctate (1) (*CI* = 0.500) Accessory Publication – Characters/Character62.pdf
(*63*) ♂ ♀ *Pronotal anterior margin*: straight (0); excavated (1); slightly bulging anteriorly (2) (*CI* = 1.000) Accessory Publication – Characters/Character63.pdf
(*64*) ♂ ♀ *Pronotal posterior margin*: straight (0); slightly indented medially (1); sharply incised medially (2) (*CI* = 1.000) Accessory Publication – Characters/Character64.pdf
(*65*) ♂ ♀ *Pronotal posterior margin lateral sinuation*: not sinuate (0); sinuate (1) (*CI* = 1.000) Accessory Publication – Characters/Character65.pdf
(*66*) ♂ ♀ *Pronotal basolateral setal denticle*: absent (0); present (1) (*CI* = 1.000) Accessory Publication – Characters/Character66.pdf
(*67*) ♂ ♀ *Pronotal median longitudinal sulcus*: lightly impressed (0); deeply impressed (1) (*CI* = 0.333) Accessory Publication – Characters/Character67.pdf
(*68*) ♂ ♀ *Pronotal basal angle*: 110° (0); 115° (1); 120° (2); 135° (3) (*CI* = 1.000) Accessory Publication – Characters/Character68.pdf
(*69*) ♂ ♀ *Pronotal lateral margin of pronotum near seta*: rounded (0); flattened curve (1) (*CI* = 0.500) Accessory Publication – Characters/Character69.pdf
(*70*) ♂ ♀ *Pronotal basal foveal macrosculpture*: not wrinkled, sparsely covered with small, fine punctures (0); not wrinkled, densely covered with large punctures (1); wrinkled and sparsely covered with medium-sized punctures (2); wrinkled with 3–4 medium-sized punctures that are usually obliterated by the wrinkles (3) (*CI* = 0.600) Accessory Publication – Characters/Character70.pdf
(*71*) ♂ ♀ *Pronotal side macrosculpture*: smooth, sparsely covered with fine punctures posterolaterad (0); covered with medium-sized punctures laterad (1); smooth, some wrinkles posterolaterad (2); smooth, some wrinkles laterad (3) (*CI* = 0.750) Accessory Publication – Characters/Character71.pdf
(*72*) ♂ ♀ *Pronotal anterior transverse impression macrosculpture*: impunctate (0); wrinkled (1); covered with medium-sized punctures (2); sparsely covered with medium-sized and fine punctures (3) (*CI* = 0.600) Accessory Publication – Characters/Character72.pdf
(*73*) ♂ ♀ *Elytral shape*: ovate (0); subparallel (1); parallel (2) (*CI* = 1.000) Accessory Publication – Characters/Character73.pdf
(*74*) ♂ ♀ *Basal region of elytra (planation/slope)*: elytral bases near middle convex, not forming gutter for reception of pronotum (0); elytral bases near middle concave, forming gutter for reception of pronotum (1) (*CI* = 1.000) Accessory Publication – Characters/Character74.pdf
(*75*) ♂ ♀ *Impression of elytral microsculpture*: shallow (0); deep (1) (*CI* = 0.250) Accessory Publication – Characters/Character75.pdf
(*76*) ♂ ♀ *Curvature of protibiae*: straight (0); curved (1) (*CI* = 1.000) Accessory Publication – Characters/Character76.pdf
(*77*) ♂ ♀ *Curvature of metatibiae*: straight (0); curved (1) (*CI* = 1.000) Accessory Publication – Characters/Character77.pdf
(*78*) ♂ ♀ *Metatrochanter shape*: rounded (0); weakly pointed (1); strongly pointed (2) (*CI* = 0.667) Accessory Publication – Characters/Character78.pdf
(*79*) ♂ ♀ *Profemoral armature*: simple (0); dorsally angulate or dentate ~1/3 from base (1); dorsally tuberculate or angulate near middle (2) (*CI* = 1.000) Accessory Publication – Characters/Character79.pdf
(*80*) ♂ ♀ *Shape of metepimeron*: ax-shaped (0); band-like, uniform width (1); band-like, width greater proximally (2); teardrop-shaped (3) (*CI* = 0.750) Accessory Publication – Characters/Character80.pdf
(*81*) ♂ ♀ *Metepisternum macrosculpture*: evenly covered with large punctures (0); evenly covered with medium-sized punctures (1); smooth (2) (*CI* = 1.000) Accessory Publication – Characters/Character81.pdf
(*82*) ♂ *Aedeagal apex shape*: similar to a rounded equilateral triangle (0); tip acuminate (1); right side incurved (2); tip square (3) (*CI* = 0.750) Accessory Publication – Characters/Character82.pdf
(*83*) ♂ *Aedeagal basal curvature*: weakly curved (0); curved (1) (*CI* = 1.000) Accessory Publication – Characters/Character83.pdf
(*84*) ♂ *Aedeagal apical bend*: straight (0); bent dorsally (1) (*CI* = 1.000) Accessory Publication – Characters/Character84.pdf
(*85*) ♂ *Apical copulatory piece (acp) twist*: acp twisted 0× (0); acp twisted 2× (1); acp twisted 3× (2) (*CI* = 0.667) Accessory Publication – Characters/Character85.pdf
(*86*) ♂ *Apical copulatory piece length*: endophallic sac twice the size of acp (0); endophallus sac 1.25× size of acp (1); acp subequal in length to endophallic sac (2) (*CI* = 0.500) Accessory Publication – Characters/Character86.pdf
(*87*) ♂ *Apical copulatory piece basal shape*: flat (0); pear-shaped (1) (*CI* = 1.000) Accessory Publication – Characters/Character87.pdf
(*88*) ♂ *Apical copulatory piece distal portion I*: distal projection absent (0); distal projection present (1) (*CI* = 1.000) Accessory Publication – Characters/Character88.pdf
(*89*) ♂ *Apical copulatory piece distal portion II*: not pointed distally (0); pointed distally (1); spoon-shaped distally (2) (*CI* = 1.000) Accessory Publication – Characters/Character89.pdf
(*90*) ♂ *Apical copulatory piece shape*: flattened, tongue-shaped (0); elongate, spear-shaped (1) (*CI* = 1.000) Accessory Publication – Characters/Character90.pdf
(*91*) ♂ *Apical copulatory piece attachment*: short, appressed to the endophallus (0); long, extended from the endophallus (1) (*CI* = 1.000) Accessory Publication – Characters/Character91.pdf
(*92*) ♀ *Gonocoxite I*: slender, lightly sclerotised (0); robust, heavily sclerotised (1) (*CI* = 0.500) Accessory Publication – Characters/Character92.pdf
(*93*) ♀ *Accessory gland*: long, narrow, length subequal to length of spermatheca (0); medium, length equal to half the length of spermatheca (1); super-long, narrow, length equal to 8–10× the length of the spermatheca (2); short, length approx. equal to 1/10 the length of the spermatheca (3) (*CI* = 1.000) Accessory Publication – Characters/Character93.pdf
(*94*) ♀ *Spermatheca*: elongate-bulb (0); filiform (1); moniliform (2) (*CI* = 0.667) Accessory Publication – Characters/Character94.pdf
(*95*) ♀ *Bursal sclerite (female)*: flat (0); domed (1) (*CI* = 0.500) Accessory Publication – Characters/Character95.pdf
(*96*) ♀ *Bursal sac*: distinctly widened near opening to vestibular chamber and below ring sclerite (0); same width from near opening of vestibular chamber to bottom of ring sclerite, or only slightly wider apically (1) (*CI* = 1.000) Accessory Publication – Characters/Character96.pdf
(*97*) ♀ *Sclerotisation of bursa copulatrix*: scattered sclerotised bodies absent (0); scattered sclerotised bodies present (1) (*CI* = 0.500) Accessory Publication – Characters/Character97.pdf

values across all the species. We calculated character state transistion cost as the difference between the range standardised median ratio values between species. For example, the median ratio values of males MXPW/VW (maxillary palpus width/vertex width) for *D. aterrimus* (*n* = 21) and *D. californicus* (*n* = 23) are 0.1086 and 0.1031, respectively. The maximum and minimum median ratio values across all species are 0.0887 and 0.1234. Using the equation above to range standardise these values, we get 576 and 415 (truncated to the nearest integer value), respectively. These values are proportional to the species median ratio value. The step matrix cost for a transition from the median ratio value of *D. aterrimus* (character state '5' = 576) to *D. californicus* (character state '3' = 415) is the difference between the values, 161—a value proportional to the gap between the species median ratio values.

We combined qualitative characters with quantitative characters using 'between-character scaling' (Wiens 2001). This procedure gives a weight of 999 to all qualitative characters and a weight of one to all quantitative characters (i.e. those characters with a maximum step-matrix transition cost of 999) in order to confer equality between them.

We therefore treated the qualitative morphological dataset as two independent character suites analysing them simultaneously: *1*, male quantitative characters (characters 1–31), and *2*, female quantitative characters (characters 32–56). This approach was due to sexual dimorphism in *Diplous*. For example, the ratio between the left metatrochanter length and the left metafemur length (male character 17 and female character 48) in *D. californicus* had median values of 0.895 in males and 0.507 in female; this is because of greatly enlarged male metatrochanters. Because the median ratio values were sometimes quite divergent (as the metatrochanter), we felt that treating males and females separately provided greater resolution to character state coding using step-matrix gap weighting. This treatment assumes independence and an equal probability of contribution between characters. This is a presumption of character state coding in any morphological phylogenetic analysis under parsimony, a model of character evolution that incorporates no explicit predefined model.

We used MacClade 4.0 to create the morphological character matrix (Appendix 2; see nexus file 'Diplous_MORPHOLOGY' in Accessory Publication – Data on the *Invertebrate Systematics* website). Range standardised species median ratio values were assigned a character state between 0–8. After the matrix was created, we exported it to PAUP*. We treated the characters according to step-matrix gap weighting and between-character scaling. Missing characters were treated as unknown. We prompted PAUP* to evaluate all possible trees in an exhaustive search using parsimony as the optimisation criterion. We performed a bootstrap and jackknife analysis of the data using a 'closest' taxon addition sequence with 1000 replicates.

Analyses of sequence data

We included at least two specimens for each of the four North American species of *Diplous* (Table 1). We used two specimens of *Qiangopatrobus* sp. to root the ingroup taxa (Table 1).

We used MacClade 4.0 to create a nexus matrix file of the aligned sequences (see nexus file 'Diplous_MOLECULES' in Accessory Publication – Data on the *Invertebrate Systematics* website). We first evaluated the trees under a branch-and-bound parsimony search, then sampled 1 000 000 trees equiprobably from the tree length–frequency distribution of all possible trees to examine skewness. We used PAUP*-employed maximum likelihood to evaluate tree topologies in order to incorporate empirically derived models of nucleotide substitution (Felsenstein 1981). In order to find the tree that best represented our data, we used the likelihood ratio test (LRT). Using the LRT, we rejected sequentially arranged models until we arrived at the model that best fitted the data and initial topology, without being overly complex (Huelsenbeck and Crandall 1997). The GTR (general time reversible) + Γ (gamma) model was the best fit for the data and the topology (Lanave *et al*. 1984; Tavaré 1986; Rodríguez *et al*. 1990). (The initial topology was the most parsimonious branch-and-bound tree.) The maximum likelihood tree was calculated from the parameters estimated from the GTR + Γ model using a heuristic search with 10 random addition replicates. We also performed a bootstrap analysis on the best-fit model of sequence evolution through an 'as-is' taxa addition sequence with 1000 replicates. We also tested the molecular clock hypothesis. We compared GTR + Γ to GTR + Γ + molecular clock using the likelihood ratio test.

Total evidence analysis

In MacClade 4.0, we combined the morphological and molecular datasets by appending the morphological dataset, including the taxa that we did not have sequence data for (*D. depressus*, *D. sibiricus caligatus*, *D. davidis*, and *D. sciakyi sciakyi*) to the beginning of the molecular dataset and filling in the empty regions with missing data (because multiple sequences were used for each species in the molecular dataset while only one terminal for each species was used in the morphological dataset; see nexus file 'Diplous_TE' in Accessory Publication – Data on the *Invertebrate Systematics* website). PAUP* evaluated the trees under a heuristic parsimony search using a 'random' addition sequence and TBR branch swapping. The characters were treated the same way as in the morphological analysis: step-matrix gap weighting of the quantitative characters with between-character scaling to give the quantitative, qualitative and sequence characters equal weight. We gave sequence characters (translated into the states: 0, 1, 2, 3) and qualitative characters a weight of 999 and the quantitative characters a weight of one. We also performed a bootstrap analysis with 369 replicates and jackknife analysis with 344 replicates using a 'closest' addition sequence.

Results of phylogenetic analyses

Morphology

Of 97 morphological characters examined, 90 were parsimony informative. The PAUP* analysis resulted in one most parsimonious tree, with a length of 191 063 steps, *CI* = 0.664, and *RI* = 0.527. The tree length distribution of all possible trees (skew, $g_1 = -0.596$) was statistically more structured ($P < 0.01$) than random data when compared to g_1 critical value (Hillis and Huelsenbeck 1992). We ran bootstrap and jackknife analyses of the data and superimposed the results onto the most parsimonious reconstruction (Fig. 3). This tree consisted of the following arrangement: (((*Qiangopatrobus* sp.+ *D. davidis*) + *D. sibiricus caligatus*) + (*D. sciakyi sciakyi*) + (*D. depressus* + (*D. rugicollis* + (*D. aterrimus* + (*D. filicornis* + *D. californicus*))))).

Sequence data

COI

Of 458 sequence characters, 409 were constant, five variable characters were parsimony uninformative, and 44 were parsimony informative. Of the 44 parsimony informative characters, 35 were localised to the 3rd position and nine to both the 1st and 2nd positions. The sequences were A–T rich with significant base frequency homogeneity across taxa. With constants removed, the base composition bias (calculated: $2/3 \times [|A - 0.25| + |C - 0.25| + |G - 0.25| + |T - 0.25|]$ (Irwin *et al*. 1991)) was somewhat high (0.381 – with 0 being no bias at all and 1 being severely biased to all one base),

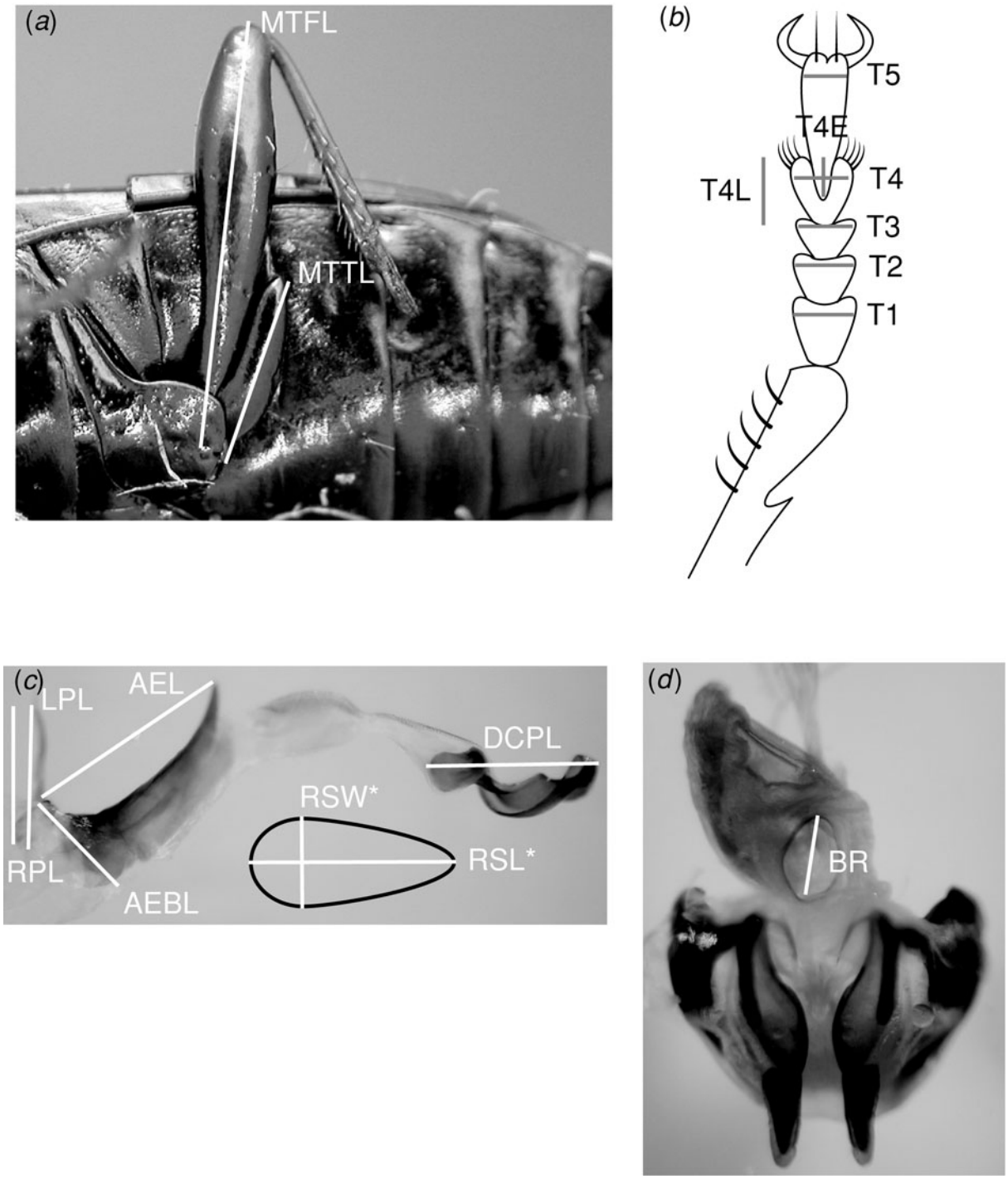

Fig. 2. Morphometries from which ratios were calculated. (*a*) Measurements of the left metafemur and metatrochanter, ventral view (MTFL, left metafemur length; MTTL, left metatrochanter length). (*b*) Measurements of tarsomeres 1–5, dorsal view (T1, left protarsomere 1 width; T2, left protarsomere 2 width; T3, left protarsomere 3 width; T4, left protarsomere 4 width; T5, left protarsomere 5 width; T4E, left protarsomere 4 emargination; T4L, left protarsomere 4 length). (*c*) Measurements of the male genitalia, lateral view (AEL, male aedeagal length (*sensu* Ball 1972); AEBL, male aedeagal base length (*sensu* Zamotajlov 1996); LPL, male left paramere length; RPL, male right paramere length; RSW, male ring sclerite width; RSL, male ring sclerite length; DCPL, male distal copulatory piece length); * depiction of male ring sclerite. (*d*) Measurements of the female genitalia, dorsal view (BR, female bursal ring width).

though expected with insect sequence A–T richness. Using a branch-and-bound search algorithm, one most parsimonious tree was obtained (L = 57; CI = 0.930; RI = 0.956). This tree had the same topology as the maximum likelihood tree (see below). The tree length distribution of 1 000 000 trees sampled equiprobably from the set of all possible trees (skew, g_1 = –1.595558) was statistically more structured ($P < 0.01$) than random data when compared to g_1 critical value (Hillis and Huelsenbeck 1992).

Likelihood ratio test

The GTR + Γ model estimated base composition, nucleotide substitution ratios, and Γ-shape. The tree presented is a single maximum likelihood phylogram with bootstrap values superimposed above supporting branch lengths (Fig. 4). This tree consisted of the following arrangement: (*Qiangopatrobus* sp. specimens+ (*D. rugicollis* specimens + (*D. californicus* specimens + (*D. filicornis* specimens + *D. aterrimus* specimens)))).

Molecular clock

In the log likelihood ratio test (H_o: GTR + Γ+molecular clock; H_a: GTR + Γ), we failed to reject the alternate hypothesis (H_a). GTR + Γ was not significantly different from the null hypothesis, GTR + Γ +molecular clock (–2lnΛ = 5.498; df = 12; P = 0.939). The nucleotides are thus assumed to have evolved in a clock-like manner. Because there are no adequate fossils for calibrating the clock, we could only calculate a local clock, or relative divergence times.

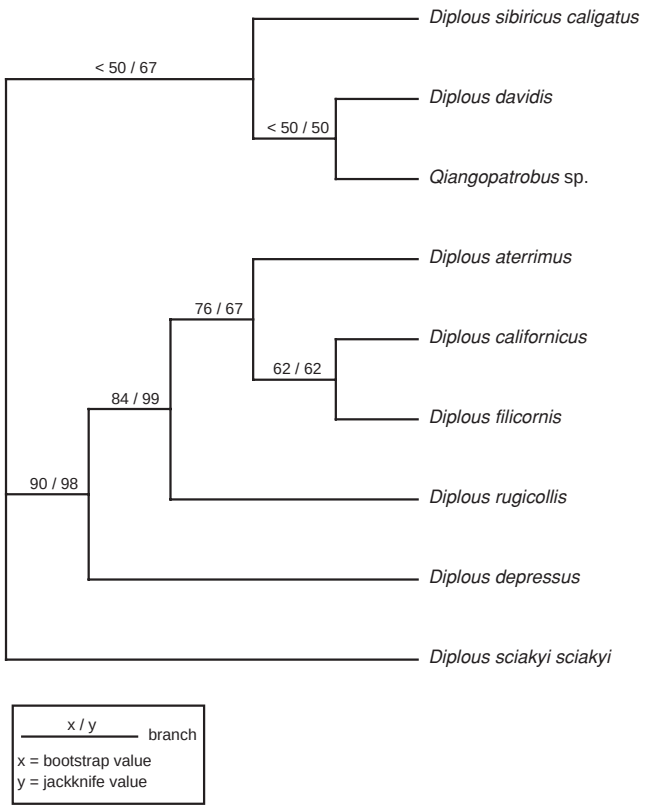

Fig. 3. Most parsimonious cladogram for the morphological dataset. Length = 191 063 steps; CI = 0.664; RI = 0.527.

Total evidence analysis

Of a combined total of 555 sequence and morphological characters, 409 were constant, 12 were parsimony uninformative, and 134 were parsimony informative. The PAUP* analysis resulted in 27 most parsimonious trees, each with a length of 250 999 steps, CI = 0.716, and RI = 0.686. We set PAUP* to create a strict consensus tree to account for differences between the 27 most parsimonious reconstructions (Fig. 5). We also ran a bootstrap and jackknife analysis of the data and superimposed the results onto the strict consensus of the most parsimonious reconstructions. This tree consisted of the same arrangement as the most parsimonious tree and the maximum likelihood tree using the molecular dataset (excluding the taxa that we did not have sequence data for, *D. depressus*, *D. sibiricus caligatus*, *D. davidis*, and *D. sciakyi sciakyi*): (*Qiangopatrobus* sp. + *D. davidis* + *D. sibiricus caligatus* + *D. sciakyi sciakyi* + *D. depressus* + (*D. rugicollis* + (*D. californicus* + (*D. filicornis* + *D. aterrimus*))))).

Discussion

Morphological and molecular trees

Though more rigorously tested in the phylogenetic analysis derived from the morphology dataset, which included more outgroup taxa, all the phylogenies supported a monophyletic North American clade. In the most parsimonious tree based on the morphology dataset, the Palearctic species, *D. depressus* was recovered as the sister-taxon to the monophyletic North American species. The most parsimonious morphology tree supports the following species relationships: (((*D. filicornis* + *D. californicus*) + *D. aterrimus*) + *D. rugicollis*). The maximum likelihood molecular tree supports the following species relationships (the position of *D. californicus* is swapped with *D. aterrimus*): (*D. filicornis* + *D. aterrimus*) + *D. californicus*) + *D. rugicollis*). The most parsimonious morphological tree and the maximum likelihood tree agree in topology, apart from the placement of *D. californicus*. These dissimilar results suggest different evolutionary histories. Although both are plausible, we are more inclined to accept the GTR + Γ maximum likelihood tree than the most parsimonious tree for three reasons.

First, the most distinctive species, *D. californicus*, may not be accommodated well by the morphological parsimony analysis. From a morphological standpoint, taking into account the total number of characters that change on the *D. californicus* branch in our phylogenetic tree and its radically different gestalt in relation to the other North American *Diplous*, *D. californicus* appears to have undergone rapid morphological divergence. Accelerated morphological diver-

gence in a single terminal taxon can make the identification of homologous structures difficult. Accelerations in morphological divergence, as in sequence divergence, often can confound the development of unequivocal hypotheses of phylogenetic relationship among species (Hansen and Martins 1996). In the most parsimonious reconstruction derived from the morphological dataset, the total number of characters that change on the internode shared between *D. filicornis* and *D. californicus* are few (37) while those on the *D. californicus* branch are many (64). Rapid morphological divergence may have resulted in character states so different that homologies cannot be recognised, resulting in the optimisation of a large number of autapomorphic characters onto the tree and possibly even an erroneous reconstruction.

Second, other taxa display similar geographical vicariance patterns among included species. That is to say, the geographical pattern of phylogenetic relationships is not unique, but rather a common one. See below for further discussion.

Third, *D. filicornis* and *D. aterrimus* share significant characters. A sister-group relationship between *D. filicornis* and *D. aterrimus* has 35 total characters that change on the branch. Six synapomorphies on this internode are 'good characters' in a classical taxonomy sense. The neck constrictions of this species-pair are deeply impressed (character 59: state 2); the pronotal basal angles are 135º (c68:s3); the pronotal anterior transverse impression macrosculpture is sparsely covered with medium-sized and fine punctures (c72:s3); the profemora are dorsally angulate or dentate ~1/3 from the apex (c79:s1); the shape of the metepimera are band-like with a width greater proximally (c80:s2); and the metepisterna macrosculpture is evenly covered with medium-sized punctures (c81:s1). On the internode between *D. filicornis* and *D. californicus* in the most parsimonious morphological tree, 37 total characters change, but only two of these characters are synapomorphies: the pronotal basolateral setal denticles are present (c66:s1) and the apical copulatory piece distal portions are spoon-shaped distally (c89:s2).

The morphological parsimony tree constrained to have *D. filicornis* and *D. aterrimus* as sister-groups is 2993 steps longer than the most parsimonious tree (191 063 to 194 056). To compare the two trees, we performed a Shimodaira-Hasegawa test (Shimodaira and Hasegawa 1999) between the morphological and molecular topologies. The Shimodaira-

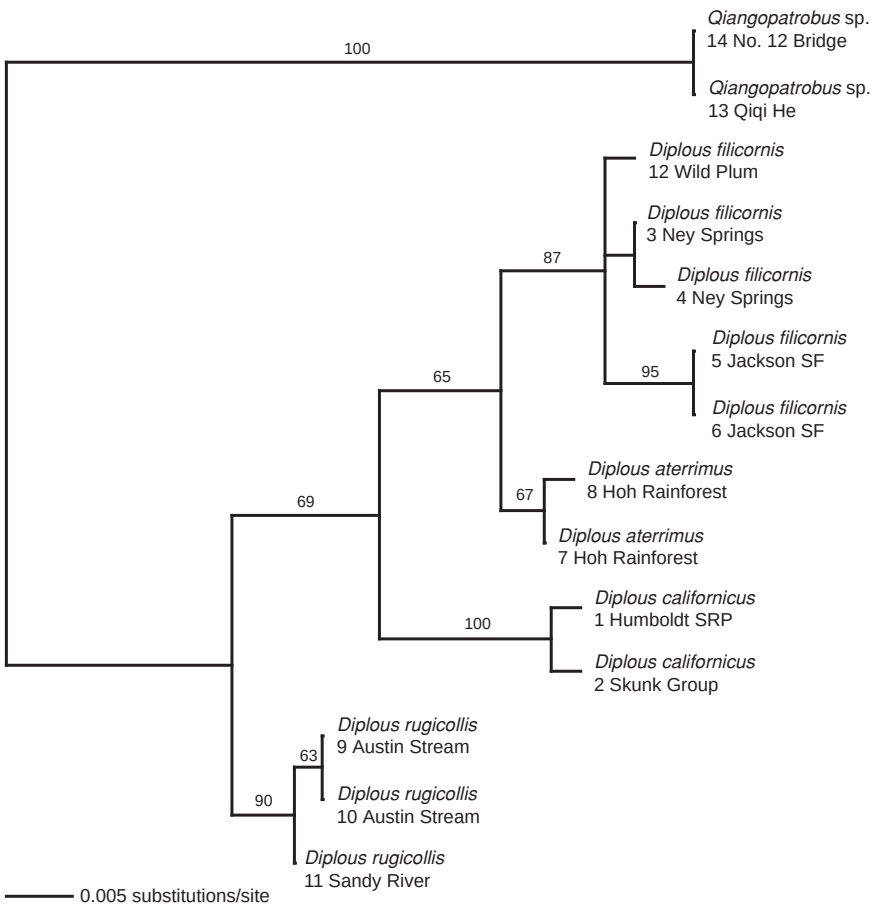

Fig. 4. Maximum likelihood phylogram for the molecular dataset (model GTR + Γ). –LnL = 927.756; bootstrap values above the branches; specimen number and shortened locality name beneath taxon names (see Table 1 for exact locality data).

Hasegawa tests an optimal topology with a suboptimal topology by examining their RELL bootstrapped log-likelihood values and comparing them based on a known distribution. In this test, the null hypothesis (H_o) is that both topologies are equally good explanations of the data while the alternate hypothesis (H_a) is that the maximum likelihood molecular topology differs significantly with the morphological topology in explanatory power of the data ($\alpha = 0.05$, one tailed test). We failed to reject the null hypothesis with a *P* value greater than 0.05 (molecular –lnL = 927.756; morphological = 933.398; $P = 0.095$).

The parsimony criterion appears to recover incorrect phylogenies when dealing with groups in which included taxa are diverging at different rates (Hansen and Martins 1996). *Diplous californicus* presents this problem: severe allometric growth (e.g. greatly enlarged metatrochanters and bilateral asymmetry) and apparent overall rapid divergence in the majority of its characters.

A special case that begs for more examination arises from our study of a population of *D. filicornis* that occurs sympatrically with a population of *D. aterrimus* that is polymorphic for genitalic characters. One population of *D. filicornis*, occurring in the Salmon River Valley in central Oregon, bears a distal copulatory piece intermediate between the highly sclerotised form of *D. aterrimus* and the lightly sclerotised form of *D. filicornis*. This may be evidence of hybridisation between *D. filicornis* and *D. aterrimus*. While this provides further support for close relationship, if not conspecificity, between *D. aterrimus* and *D. filicornis*, further investigations, both from a molecular and morphological perspective, are needed.

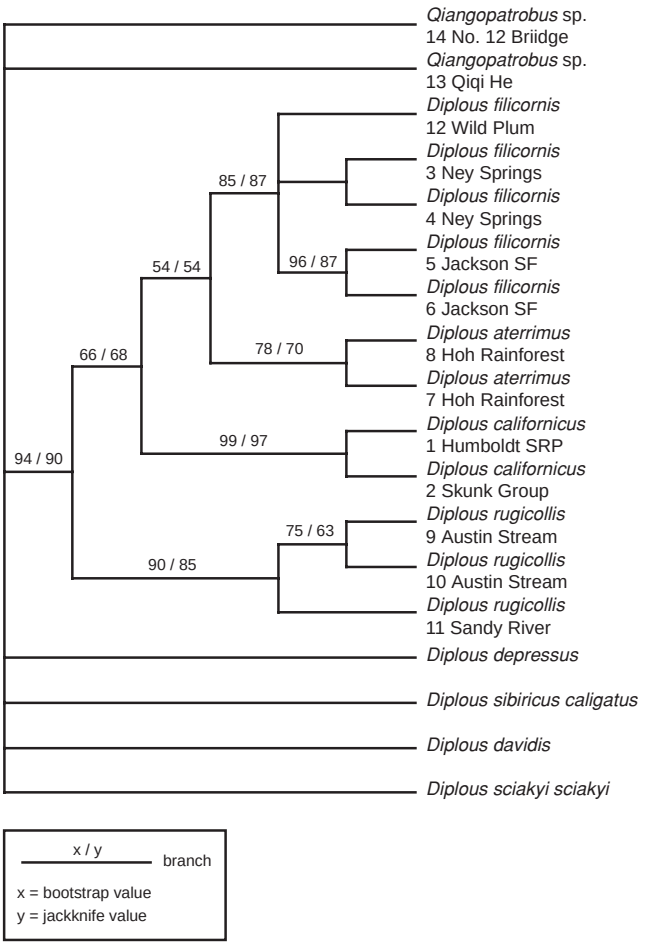

Fig. 5. Maximum parsimony consensus cladogram for the total evidence dataset. Length, 250 999 steps; *CI* = 0.716; *RI* = 0.686.

Biogeography

Origins of Diplous *in North America*

As a result of comparing the phylogeny of the North American *Diplous* with its distribution and with the distributions of its most closely related taxa, the genus likely originated from a widespread northern ancestor. This is consistent with other studies (Hoffman 1963, *Hypochilus* spiders; Shelley 1993, *Scytonotus* millipedes; Wooding and Ward 1997, *Ursus* bears; Wen 1999, flowering plants), which show elements of the fauna of the Pacific north-west and trans-North America descended from widespread northern Laurasian warm temperate Tertiary ancestors (Fig. 6*a*) that have been shaped by a series of vicariant events (mostly glaciation and/or drying) beginning in the mid-Tertiary and reaching its maximum during the Pleistocene (Kavanaugh 1988). The most parsimonious tree based on morphology (Fig. 3) suggests that *D. depressus* is the sister taxon to the Nearctic species. It is also geographically adjacent to the Nearctic fauna, ranging from the Kuril Islands in the east to the Xinjiang Province of China in the west. It also shares important genitalic features (*D. depressus* shares a similar distal copulatory piece with the North American *Diplous*).

Phylogenetic considerations within a biogeographical context

According to the preferred phylogeny of North American *Diplous*, three speciation events occurred. Each of these events may have been associated with a glacial event. The first split, between the western and eastern species, is concordant with the southward expansion of glaciers in central North America or the drying of central North America to create the Great Plains. The disjunction between eastern and western species is due most likely to a combination of glaciation, absence of glacial refugia with suitable habitats in central North America, subsequent drying to create the Great Plains, and the absence of fast-flowing, gravelly or rocky streams in that region. *Diplous rugicollis* or the ancestral North American *Diplous* in the east could have survived in glacial refugia in the southern Adirondacks or northern Appalachian Mountains or possibly slightly further south in the Appalachian range. The ancestral western *Diplous* may have survived in glacial refugia in the southern Rocky Mountains and/or the Pacific coast (Fig. 6*b*). Although the

molecular clock hypothesis was not significantly different from the null model and therefore not rejected, fossil evidence for *Diplous* does not exist, so any theories about absolute age of the speciation events and subsequently correlation between glaciation events will not be attempted. The percent difference between the eastern and western clades in uncorrected p-distance is ~3%, which corresponds to a relative age of ~1.3–2.0 million years (using 2.3% (Brower 1994) and 1.5% (Quek *et al*. 2004) per million year divergence rates for arthropod mtDNA respectively; the latter, more conservative rate estimate, is probably more accurate because it was calculated using primarily *COI* sequence data whereas the former rate was calculated using a large portion of *COII* sequence). After the initial glaciation that isolated the eastern and western taxa started to recede, the ancestors of *D. rugicollis* and the common ancestor of *D. californicus* + *D. aterrimus* + *D. filicornis* may have started to expand northward (Fig. 6*c*). Several mammalian taxa with distinct eastern and western North American clades exhibit similar divergence: martens, 2.5–3.0%, cyt b (Stone *et al*. 2002); and black bears, 3.3% cyt b (Wooding and Ward 1997).

The second split may reflect the results of a second glacial period that isolated the common ancestor of *D. aterrimus* and *D. filicornis* in the southern Rocky Mountains and the ancestors of *D. californicus* in the southern Pacific coastal

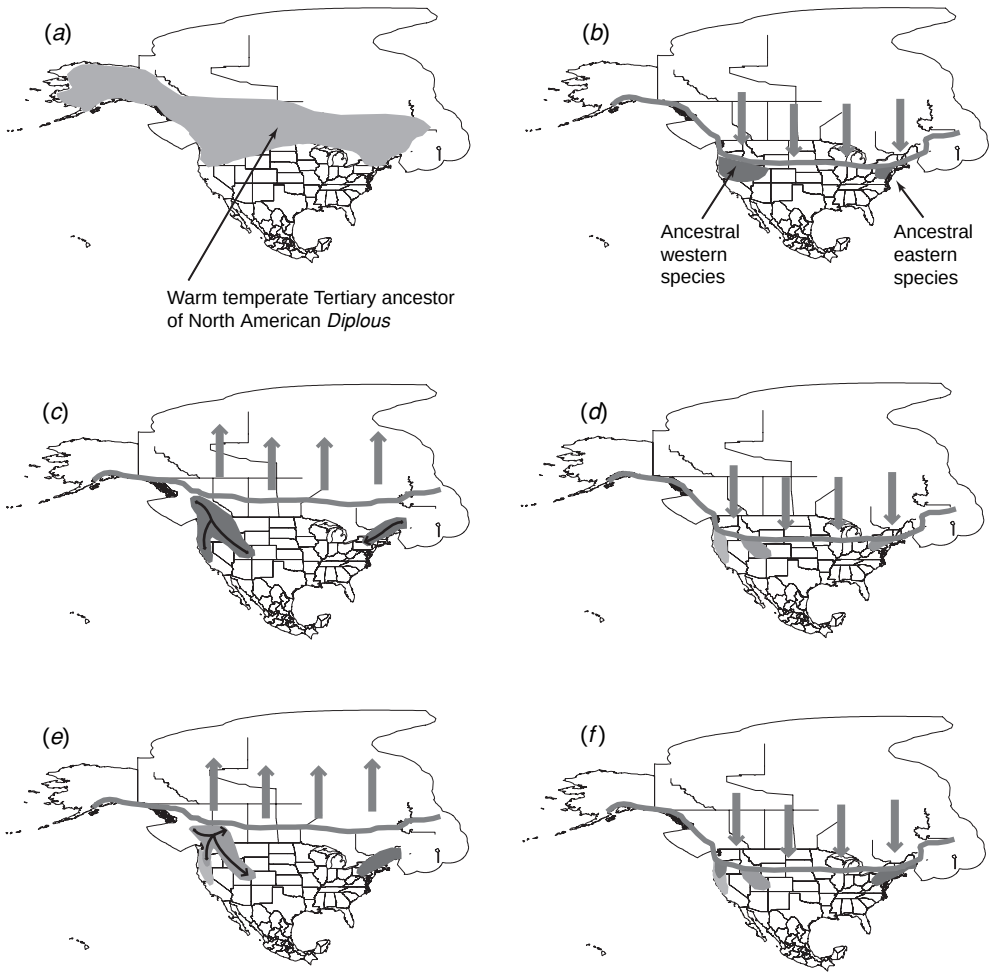

Fig. 6. Proposed glaciation/cooling scenario for the speciation of North American *Diplous*. (*a*) Widespread northern ancestor; (*b*) southward expansion of glaciers in North America resulting in disjunction between the eastern and western ancestral species; (*c*) expansion of the ranges of the ancestor of *D. rugicollis* and the common ancestor of *D. californicus* + *D. aterrimus* + *D. filicornis* northward after warming; (*d*) second glacial period that isolated the common ancestor of *D. aterrimus* and *D. filicornis* in the southern Rocky Mountains and the ancestor of *D. californicus* in the southern Pacific coastal region; (*e*) recession of early Pleistocene glaciation and broad occupation of the western mountainous region from the Rocky Mountains to the Pacific coastal Mountains by the common ancestor of *D. aterrimus* + *D. filicornis*; (*f*) isolation by glaciation of the ancestor of *D. aterrimus* in the southern Rocky Mountains and the ancestor of *D. filicornis* in the southern Cascade and Pacific coast Mountains.

region. The divergence between the southern coastal and southern Rocky Mountain elements, like the eastern and western species, might have been reinforced by expansion of arid regions, specifically the Columbian Plateau and other Great Basin regions (Fig. 6*d*). The southern Rocky Mountains and the Pacific coast have been identified as potential glacial refugia based on mtDNA in the dusky shrew, *Sorex monticolus* (Demboski and Cook 2001), martens (Stone *et al*. 2002) and in carabid beetles (Kavanaugh 1988). Close sister-group relationships between coastal and Rocky Mountain elements have been shown in animals such as the dusky shrew (Demboski and Cook 2001), other mammals (Foster 1965), and nebriine carabid beetles (Kavanaugh 1988). With subsequent recession of this early Pleistocene glaciation, the common ancestor of *D. aterrimus* + *D. filicornis* may have been able to occupy the entire western mountainous region from the Rocky Mountains to the Pacific coastal mountains (Fig. 6*e*).

The third split appears to be a result of yet another glacial period that may have isolated the ancestor of *D. aterrimus* in the southern Rocky Mountains (again) and the ancestors of *D. filicornis* in the southern Cascade and Pacific coast Mountains (Fig. 6*f*). This relationship between Rocky Mountain species and coast-restricted species has also been shown in species of the ground beetle genus, *Nebria*, specifically in the acuta-group (Kavanaugh 1988). The common ancestor of *D. aterrimus* + *D. filicornis* was probably very similar structurally to *D. aterrimus*, judging by the branch lengths separating each from the ancestral node. Therefore, asymmetrical divergence occurred after the speciation of *D. aterrimus* + *D. filicornis* resulting in a longer branch length in *D. filicornis*. Just as with *D. californicus*, this relatively longer branch length in *D. filicornis*, may be due to similar selective pressures at work in the same region in which these two species are sympatric.

Divergence times estimated from the putative clock-like substitution rate of mtDNA may be useful to date speciation events in the Pleistocene. However, the timing of particular speciation events with specific glacial events is difficult to assess because: *1*, a large number of glacial cycles occurred in the Pleistocene; *2*, many of these events are uncorroborated by specific evidence (e.g. spatial evidence like moraine formation for inferring glacial boundaries), and *3*, speciation rates may be inconsistent with a 2.3% or 1.5% divergence/1 Myr mtDNA substitution rate. Likewise, factors influencing speciation, other than allopatric speciation by isolation/glaciation, may be operating. The appearance of the western species, *D. californicus*, with its wildly divergent morphology (64 total character states change on the terminal branch in the morphological parsimony analysis) suggests a scenario that is more consistent with speciation by natural or sexual selection rather than one by genetic drift by isolation. Therefore, relying on a speciation mechanism dependent on glaciation-driven isolation may be overly simplistic.

Taxonomy of the North American species of *Diplous*

Darlington (1938) and Lindroth (1961) revised the North American species of *Diplous*. See Darlington (1938) for further information regarding synonymies.

Genus ***Diplous*** Motschulsky

Diplous Motschulsky, 1850: 71, pl. 10.

Type species: *Patrobus sibiricus* Motschulsky, 1844: 128, pl. 6, fig. 2.

Platidius Chaudoir, 1871: 51. Type species: *Patrobus aterrimus* Dejean, 1828, by subsequent designation (Darlington 1938).

Diagnosis (Darlington 1938; Zamotajlov 1992)

Adults of *Diplous* may be differentiated from other genera in the tribe Patrobini based on the combination of: body shape flattened; eyes large, strongly convex; antennomere one with single long seta; occipital constriction shallow; postgenal length usually less than eye diameter; anterior half of pronotal margin with single seta; pronotal median longitudinal sulcus lightly impressed, diminished near base, basal part of impression never excavated into a gutter; pronotal sides strongly punctured; tarsomeres broad; pro- and mesotarsomere four wider than long, often bilobed.

The character used by Chaudoir (1871) for establishing the North American subgenus *Platidius*, namely bifid emargination of the fourth tarsal segment, is not a synapomorphy for Nearctic species in the inferred phylogeny, however, a few aedeagal characters are synapomorphies: e.g. apical copulatory piece pointed distally (*sensu* Lindroth 1961) and apical copulatory piece elongate, spear-shaped. Although we recovered a monophyletic Nearctic *Diplous*, we did not recover reciprocally monophyletic Nearctic and Palearctic clades; the Palearctic fauna is paraphyletic with respect to the North American species in the phylogeny based on morphology. The Palearctic fauna is also recovered as paraphyletic in an exemplar phylogeny of the tribe Patrobini (Zamotajlov 2002). The Nearctic species and the Palearctic species, *Diplous depressus*, are united by several synapomorphies, e.g. pear-shaped apical copulatory piece basal shape. Lindroth (1961) and Kühnelt (1941) supported a natural grouping of the Nearctic species, but they did not consider the monophyly of the Palearctic species. We feel that taxonomic names should correspond to monophyletic groups and not paraphyletic ones. Accordingly, we do not recognise the subgenus *Diplous* and, as a consequence, the subgenus *Platidius*.

Diplous aterrimus (Dejean)

Patrobus aterrimus Dejean, 1828: 32. Sex of holotype unknown, type depository unknown. Darlington (1938) wrote that the type was deposited in the Oberthür Collection (MNHN), although Lindroth (1961) reported that the types of Dejean and Chaudoir

were missing from this collection. Type locality: Norfolk Sound near Sitka, Alaska, USA (Darlington 1938).
Patrobus fulcratus (LeConte, 1869): 374.
Platidius breviceps Casey, 1918: 402.
Platidius coloradensis Casey, 1918: 403.
Platidius reflexus Casey, 1918: 403.
Platidius tenuitarsis Casey, 1918: 403.

Material examined

Canada. **British Columbia:** 1♂, 1♀, Forwards Harbour (CASC); 1♂, 1♀, Queen Charlotte Is, Graham I. (CASC); 1♂, 1♀, Vancouver I. (CASC); 1♀, Alaska Hwy Mile 594.3, Irons Creek (CASC); 1♂, Alaska Hwy Mile 687.1, Lower Rancheria River (CASC); 1♂, Nanika Lake (CASC); **North-west Territories:** 1♂, District of MacKenzie County, Aklavik (CASC); **Yukon Territory:** 1♂, 1♀, Spruce Creek, km 61.5 on Route 10 (BMNH); 1♂, 1♀, Route 4, Finlayson River (BMNH); 1♂, Route 5, Rock River, (BMNH). **USA. Alaska:** 1♂, Rudyard Bay, Nooya Lake (CASC); **Colorado:** 1♂, 1♀, Boulder County, North Saint Vrain Creek at Hwy (CASC); 1♂, Conejos County, San Juan Mts (CASC,); 1♀, San Juan County, Silverton area (CASC); **Idaho:** 1♂, 1♀, Camas County, Soldier Range (CASC); 1♂, 1♀, Clearwater County, Moose Mts (CASC); 1♀, Custer County, Salmon River Mts, Hwy (CASC); **Montana:** 1♂, 1♀, Cascade County, Little Belt Mts (CASC); 1♂, Glacier National Park, Livingstone Range (CASC); **Oregon:** 1♂, Union County, NW of Elgin (CASC); 1♂, 1♀, Wallowa County, Wallowa Mts (CASC); **Utah:** 1♂, 1♀, Wasatch County, Wasatch Range (CASC); **Washington:** 1♂, Walla Walla County, S of Walla Walla (CASC); **Wyoming:** 1♂, 1♀, Sheridan County, Bighorn Mts (CASC); 1♂, 1♀, Sublette County, Gros Ventre, (CASC).

Diagnosis

Adults of *Diplous aterrimus* are distinct from those of the other North American *Diplous* based on the combination of: mandibles, palpi, legs, and antennae black with a heavy red tint; neck constriction sparsely covered with small punctures dorsomedially; pronotal anterior transverse impression impunctate or sparsely covered with medium-sized and fine punctures (Fig. 7*a*); pronotal basal fovea wrinkled (Fig. 7*a*); elytra parallel-sided (Fig. 8*a*); elytra dull (elytral microsculpture consisting of deeply impressed isodiametric meshes (Fig. 8*b*); males with pointed and elongate metatrochanters, 0.425 to 0.600× the length of the metafemora (Fig. 8*c*); aedeagus with square apex (Fig. 9*a*); aedeagal apical copulatory piece strongly sclerotised, spear-like (Fig. 9*b*); bursal sclerite in females domed (Fig. 9*c*).

Distribution

Found mainly in the Rocky Mountain region, from southern Colorado and central Utah north to the North-west and Yukon Territories, west to eastern Oregon and Washington, and reaching the Pacific coast in British Columbia, including the Queen Charlotte Is, and south-eastern Alaska (Fig. 10).

Habitat

Riparian; large, moderately to fast flowing streams. Known elevation range: sea level to 3690 m, mean: 1519 m, $n = 145$.

Diplous californicus (Motschulsky)

Patrobus californicus Motschulsky, 1859: 123 (also in Motschulsky, 1850: 6). Sex of holotype unknown, type depository unknown. Darlington (1938) wrote that the type was deposited in the Motschulsky Collection (ZMMU). Lectotype deposited in the MCZ (Type number: 8232). Type locality: 'near San Francisco', USA.
Patrobus trochantericus (LeConte, 1869): 375.
Platidius breviusculus Casey, 1918: 401.
Platidius incisus Casey, 1918: 399.
Platidius latipennis Casey, 1918: 399.
Platidius rectus Casey, 1918: 400.
Platidius sierranus Casey, 1918: 401.
Platidius strenuus Casey, 1918: 400.

Material examined

Canada. British Columbia: 1♂, Princeton (CASC); 1♀, Midday Valley, Merritt (CASC); 1♂, Vancouver I., Robson Bight, Tsitika River (CASC). **USA. California:** 1♂, 1♀, Calaveras County, Mokelumne Hill (CASC); 1♂, 1♀, Del Norte County, Jedediah Smith State Park (CASC); 1♂, 1♀, Fresno County, S Fork of Kings River (CASC); 1♂, 1♀, Humboldt County, Korbel (CASC); 1♂, 1♀, Eel River at Richardson Grove (CASC); 1♀, Mendocino County, Eel River Ranger Station (CASC); 1♂, Middle Fork of Eel River, 0.2 km (0.3 miles) below mouth of Black Butte River (CASC); 1♀, Sonoma County, Gualala Creek (CASC); **Idaho:** 1♂, 1♀, Custer County, Salmon River Mts, Hwy 93, 16.1 km (10 miles) E of Lower Stanley (CASC); 1♂, 1♀, Elmore County, Sawtooth Mts, Soldier Range, 4.8 km (3 miles) N of Pine, S Fork Boise River at Dog Creek Campground (CASC); 1♂, Idaho County, Salmon River, 2.4 km (1.5 miles) N of Slate Creek Ranger Station (CASC); 1♀, Clearwater Mts, Selway River at mouth of O'Hara Creek (CASC); 1♂, 1♀, Nez Perce County, Hwy 12/95, 3.2 km (2 miles) E of Lewiston, Clearwater River (CASC); **Montana:** 1♂, 1♀, Mineral County, St Regis River at St Regis (CASC); **Nevada:** 1♀, Washoe County, Verdi, Truckee River (CASC); **Oregon:** 1♂, 1♀, Clackamas County, Molalla River at Hwy (CASC); 1♂, 1♀, Clatsop County, Cannon Beach (CASC); 1♂, Curry County, 3.2 km (2 miles) S of Gold Beach, at mouth of Hunter Creek (CASC); 1♀, Douglas County, Cascade Range, Steamboat Creek at Steamboat Falls (CASC); 1♀, Grant County, Blue Mts, 2.4 km (1.5 miles) E of Mt Vernon, Hwy 26, John Day River (CASC); 1♂, Jackson County, Rogue River at Touvelle State Park (CASC); 1♂, 1♀, I.5, 3.2 km (2 miles) E of Rogue River City, Rogue River (CASC); 1♀, Lane County, Cascade Range, 1.4 km (0.9 miles) W of Nimrod, McKenzie R. (CASC); 1♀, Umatilla County, Blue Mts, 1 mile N of Dale, North Fork of John Day River (CASC); 1♂, 1♀, Wallowa County, 0.3 km (0.2 miles) SE of Minam, at junction of Minam and Wallowa Rivers., Hwy 82 (CASC); **Washington:** 1♂, 1♀, Clallam County, junction of Soleduck and Bogachiel Rivers (CASC); 1♂, 1♀, Jefferson County (CASC); 1♂, 1♀, Pierce County, Cascade Range, junction of Hwys 7 706, Elbe, Nisqually River (CASC); 1♀, Whatcom County, Cascade Range, Hwy 542, 30.6 km (19 miles) W of Glacier, North Fork of Nooksack River (CASC); 1♂, Cascade Range, Hwy 542, 6.4 km (4 miles) E of Glacier, N.F. Nooksack River (CASC).

Diagnosis

Adults of *Diplous californicus* are distinct from those of the other North American *Diplous* based on the combination of: palpi, legs, and antennae black with a light-red tint; neck constriction smooth; pronotal anterior transverse impression impunctate or sparsely covered with medium-sized and fine punctures (Fig. 7*b*); sides of pronotum with wrinkles laterad

(extending from anterior margin to posterior margin (Fig. 7*b*)); pronotal basal fovea wrinkled, with three or four medium punctures that are usually obliterated by the wrinkles (Fig. 7*b*); males with very large metatrochanters, 0.760 to 1.012× the length of the metafemora (Fig. 8*c*).

Distribution

Found mainly along the Pacific coast, from the Sierra Nevada and northern Coast Ranges of California, north to Vancouver I. and south-central British Columbia, east to extreme western Nevada and across the Columbia Plateau to central Idaho and extreme western Montana (Fig. 10).

Habitat

Riparian; larger, more slowly moving streams and rivers. Known elevation range: 8.5 m to 1800 m; mean: 533.78 m, $n = 96$.

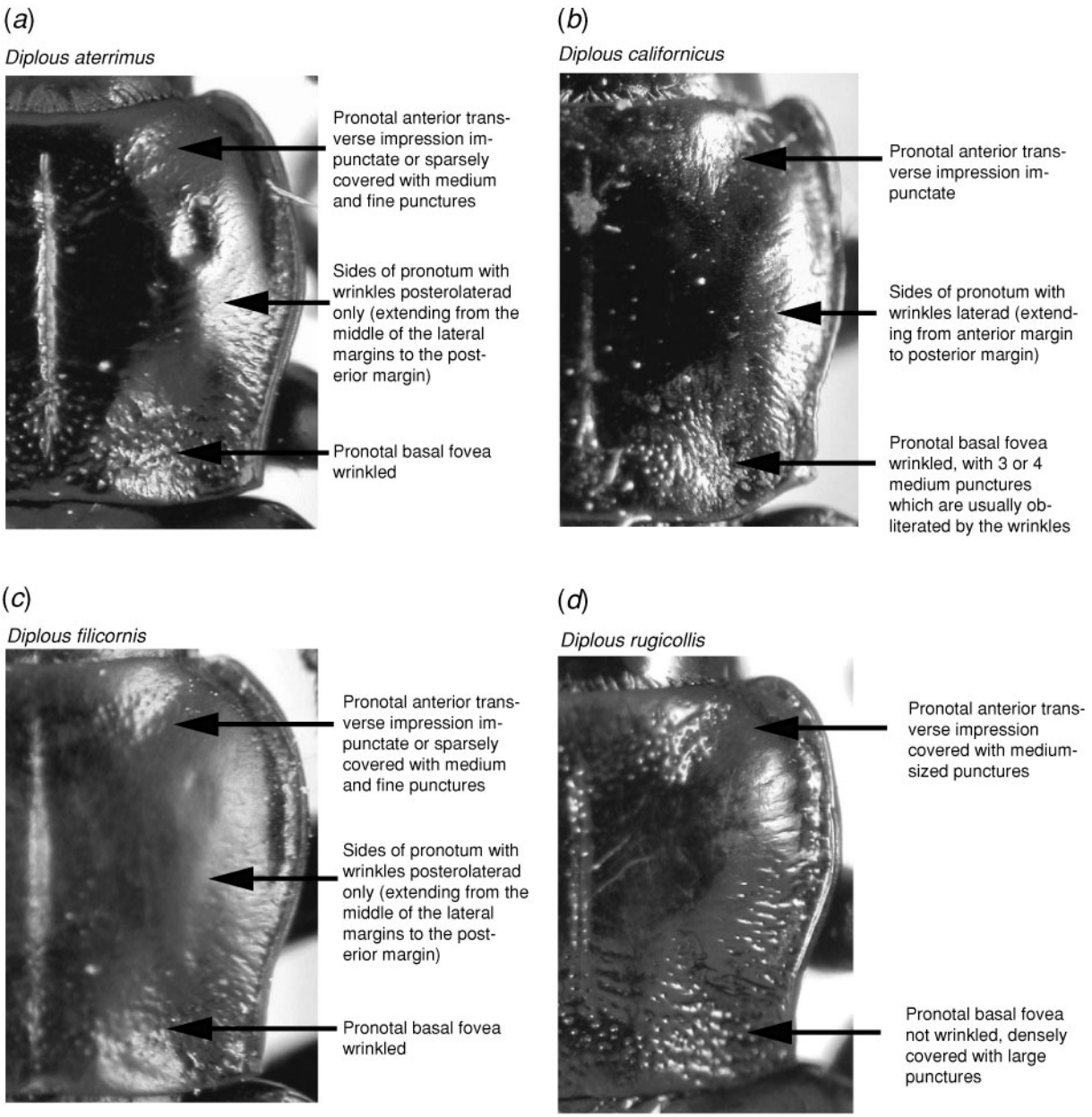

Fig. 7. Diagnostic characters of the pronotum in North American *Diplous*. Pronotal anterior transverse impression macrosculpture, sides of pronotum macrosculpture, pronotal basal fovea macrosculpture: (*a*) *Diplous aterrimus*; (*b*) *D. californicus*; (*c*) *D. filicornis*; (*d*) *D. rugicollis*.

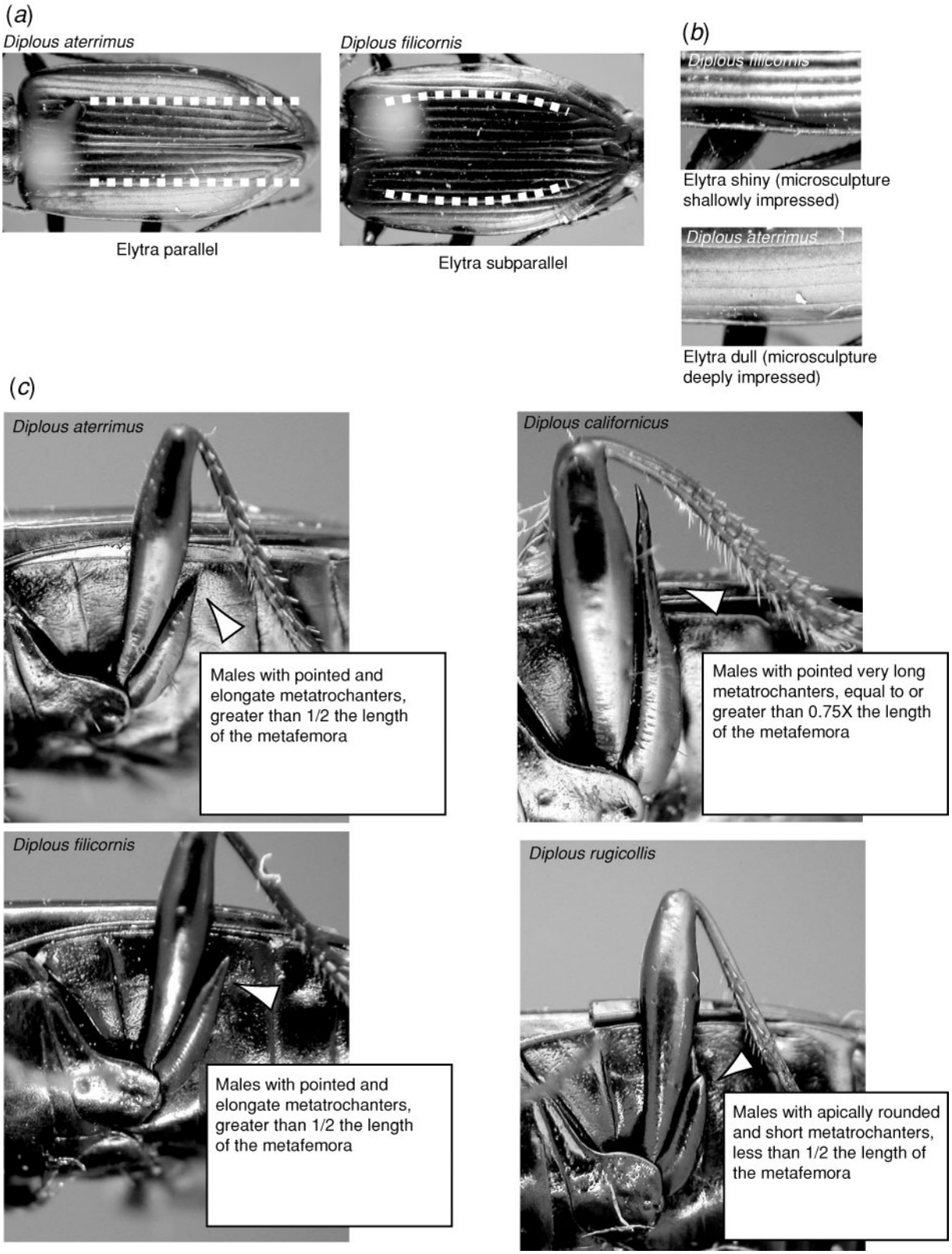

Fig. 8. Diagnostic characters of the elytra and legs in North American *Diplous*. (*a*) Elytra shape; (*b*) elytra microsculpture; (*c*) male metatrochanters shape and size.

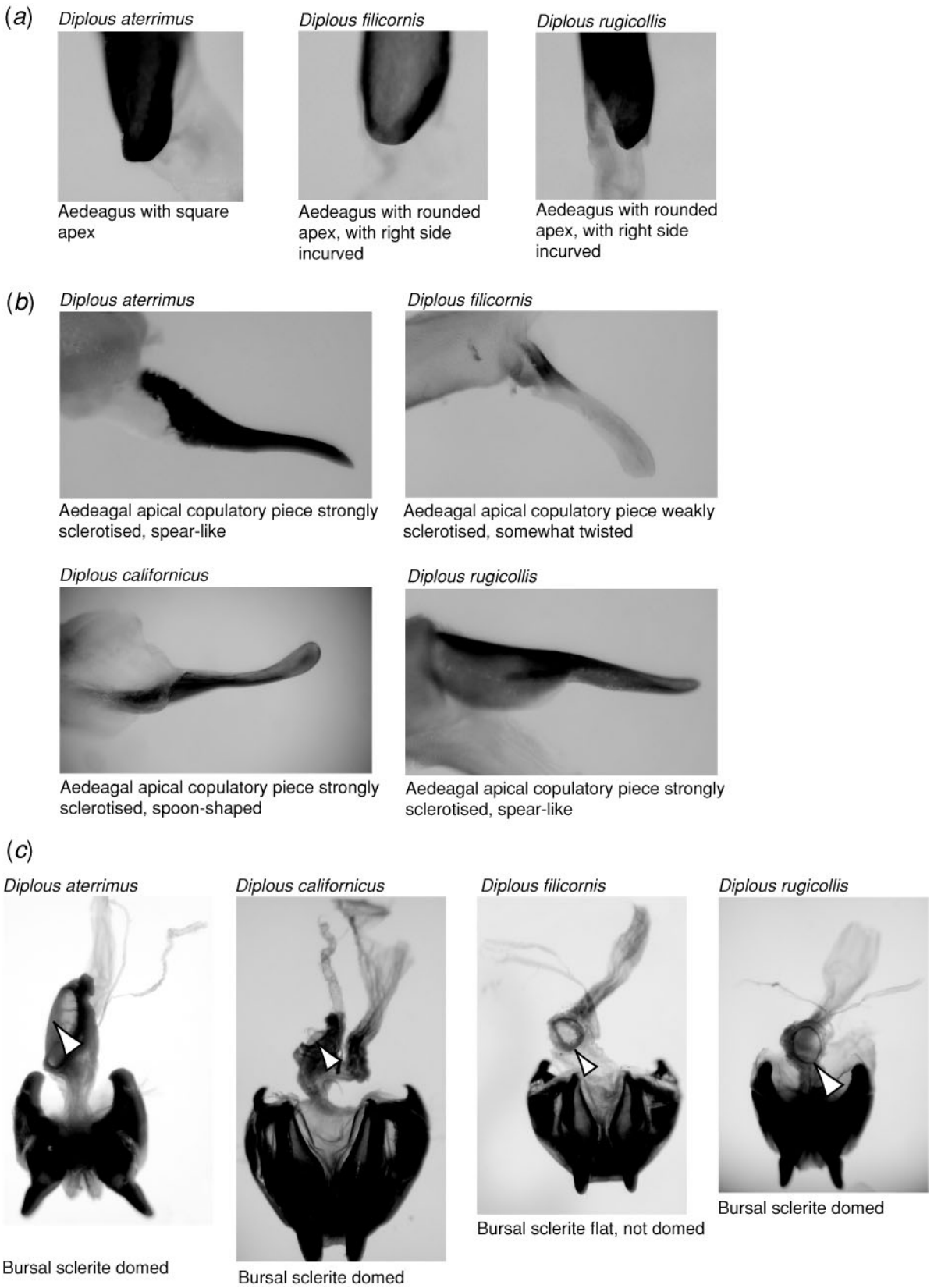

Fig. 9. Diagnostic characters of the male and female genitalia in North American *Diplous*. (*a*) Aedeagal apex shape; (*b*) aedeagal apical copulatory piece sclerotisation and shape; (*c*) bursal sclerite shape.

Diplous filicornis (Casey)

Platidius filicornis Casey, 1918: 404. Female lectotype deposited at USNM, designated by Lindroth (1975). Type locality: Redwood Creek, Humboldt Co., California, USA.

Material examined

Canada. British Columbia: 1♂, 1♀, Alice Lake Provincial Park, Cheekye River at outlet from Stump Lake (CASC). **USA. California:** 1♂, 1♀, Del Norte County, Coast Range, Hwy 199, 5.8 km (3.6 miles) SSW of Elk Valley, Griffin Creek (CASC); 1♂, Jedediah Smith State Park, Smith River at Stout Grove (CASC); 1♂, 1♀, El Dorado County, Sierra Nevada, South Fork of American River, 3.2 km (2 miles) E of Kyburz (CASC); 1♀, Plumas County, Lassen Volcanic National Park, Cascade Range, Sulfur Works area, West Sulfur Creek (CASC); 1♂, 3.7 km (2.3 miles) N of Chester, North Fork of Feather River (CASC); 1♂, 1♀, Trinity County, Trinity Alps, South Fork of Salmon River at Big Flat Campground (CASC); **Oregon:** 1♂, Douglas County, Cascade Range, junction of Steamboat Creek and North Umpqua River at (CASC); 1♀, Lane County, Cascade Range, 1.4 km (0.9 miles) W of Nimrod, MacKenzie R. (CASC); 1♂, 1♀, Cascade Range, 36.4 km (22.6 miles) SE of Oakridge on Hwy 58, Salt Creek (CASC); 1♂, 1♀, Marion County, 11.9 km (7.4 miles) W of Mill City on Hwy 22, Little North Santiam River (CASC); **Washington:** 1♂, Cowlitz County, 14.5 km (9 miles) W of Longview, under log along Columbia River (CASC); 1♂, 1♀, Pierce County, Mt Rainier National Park, Louise Lake (CASC).

Diagnosis

Adults of *Diplous filicornis* are distinct from those of the other North American *Diplous* based on the combination of: mandibles, palpi, legs, and antennae black with a heavy red tint; neck constriction sparsely covered with small punctures dorsomedially; pronotal anterior transverse impression impunctate or sparsely covered with medium-sized and fine punctures (Fig. 7*c*); pronotal basal fovea wrinkled (Fig. 7*c*); elytra subparallel to ovoid (Fig. 8*a*); elytra shiny (i.e. elytral microsculpture consisting of shallowly impressed isodia-

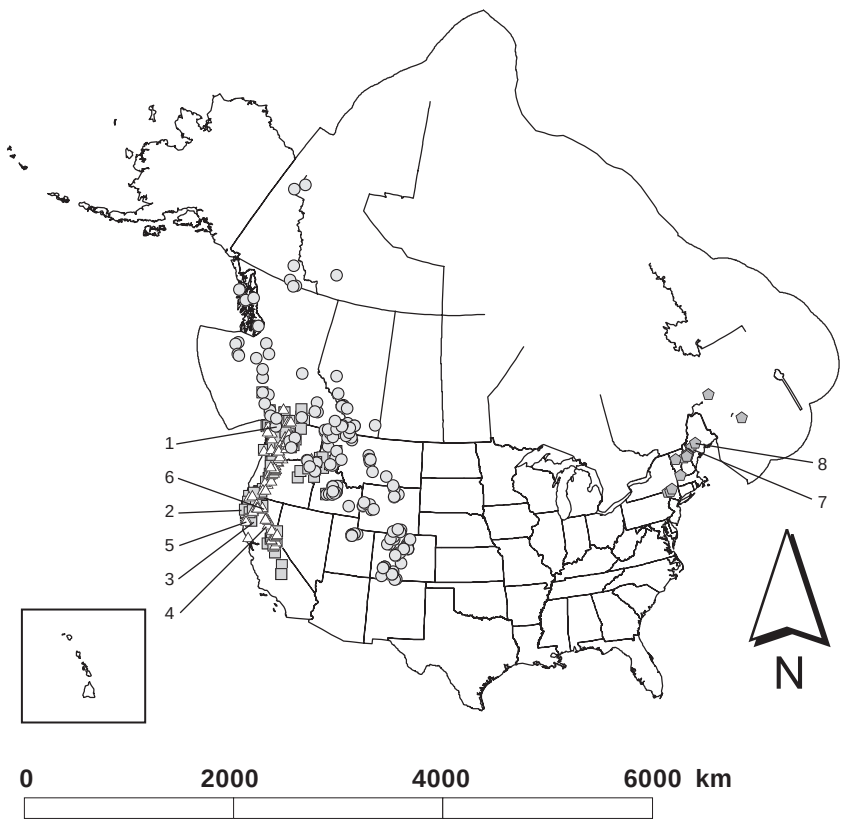

DNA specimen localities
1. *Diplous aterrimus*: Hoh Rainforest, Washington
2. *D. californicus*: Humboldt State Redwood Park, Humboldt Co., California
3. *D. californicus*: Skunk Group Campground, Trinity Co., California
4. *D. filicornis*: Wild Plum Campground, Sierra Co., California
5. *D. filicornis*: Jackson State Forest, Mendocino Co., California
6. *D. filicornis*: Ney Springs Creek, Siskiyou Co., California
7. *D. rugicollis*: Sandy River, Franklin Co., Maine
8. *D. rugicollis*: Austin Stream, Somerset Co., Maine

Fig. 10. Distribution map of North American *Diplous* Motschulsky. *Diplous aterrimus*, circles; *D. filicornis*, triangles; *D. californicus*, squares; *D. rugicollis*, pentagons. The localities of DNA specimens are indicated by numbers explained at the bottom of the figure.

metric meshes (Fig. 8*b*); males with pointed and elongate metatrochanters, 0.523 to 0.665× the length of the metafemora (Fig. 8*c*); aedeagus with rounded apex, with right side incurved (Fig. 9*a*); aedeagal apical copulatory piece weakly sclerotised, somewhat twisted (Fig. 9*b*); bursal sclerite in females flat, not domed (Fig. 9*c*).

Distribution

Found exclusively along the Pacific coast, in the Coast Ranges from northern California to the Olympic Peninsula in Washington and in the northern Sierra Nevada and Cascade Range of Oregon and Washington; also in extreme south-western mainland British Columbia (Fig. 10).

Habitat

Riparian; narrow, more quickly moving streams and rivers. Known elevation range: 22 m to 2290 m; mean: 800 m, $n = 90$.

Diplous rugicollis (Randall)

Patrobus rugicollis Randall, 1838: 560 (erratum). Male neotype deposited in the MCZ (Type number: 23357) (Darlington, 1938). Neotype locality: Groton Notch, near Bethel, Maine, USA.

Patrobus angicollis [lapsus calami] Randall, 1838: 1, pl. 1, fig. 1; pl. 3, figs 77–79.

Patrobus longipalpus Notman, 1919: 231

Material examined

Canada. Nova Scotia: 2♀, Truro (CASC); **Québec:** 1♂, 1♀, Peninsula de Gaspe, 38.6 km (24 miles) NNW of New Richmond, Cascapedia River at Ruisseau Marcil (CASC). **USA: New Hampshire:** 1♂, Coos County, road rest area on Route 2, between Gorham + Shelburn (CASC); 1♂, 1♀, Fabyan's Restaurant, Mount Washington Hotel (CASC); 1♀, Amonoosuc River, Base of Mt Washington (CASC); **New York:** 1♂, 1♀, Sullivan County, Hwy 17 at Roscoe, Willowemoc Creek (CASC); 1♂, 1♀, Ulster County, 27.4 km (17 miles) SW of Oliverea, West Branch Neversink Creek (CASC); **Vermont:** 1♂, 1♀, Chittenden County, Green Mountains, 1 mile S of North Duxbury, Ridley Brook (CASC); 1♀, Windham County, Dover, Blue Brook (CASC).

Diagnosis

Adults of *Diplous rugicollis* are distinct from those of the other North American *Diplous* based on the combination of: pronotal anterior transverse impression covered with medium-sized punctures (Fig. 7*d*); pronotal basal fovea not wrinkled, densely covered with large punctures (Fig. 7*d*); males with apically rounded and short metatrochanters, distinctly less than 1/2 the length of the metafemora (Fig. 8*c*).

Distribution

Found only in north-eastern New England and extreme south-eastern Canada, from the Adirondack Mountains of New York, the Green Mountains of Vermont, and White Mountains of New Hampshire north to Nova Scotia and the Gaspé Peninsula of Quebec (Fig. 10).

Habitat

Riparian; 'large streams in the notches or at the foot of the larger mountains' (Darlington 1938: 152). Known elevation range: 60 m to 1520 m; mean: 425.74 m, $n = 16$.

Key to the species of North American *Diplous*

1. Pronotal anterior transverse impression impunctate or sparsely covered with medium-sized and fine punctures (Fig. 7*a*,*c*); pronotal basal fovea wrinkled (Fig. 2*a*); males with pointed and elongate metatrochanters, equal to or greater than 1/2 the length of the metafemora (Fig. 8*c*). (Western species) 2
   Pronotal anterior transverse impression covered with medium-sized punctures (Fig. 7*d*); pronotal basal fovea not wrinkled, densely covered with large punctures (Fig. 7*d*); males with apically rounded and short metatrochanters, distinctly less than 1/2 the length of the metafemora (Fig. 8*c*). (Eastern species). . . . . *Diplous rugicollis* (Randall)
2. Mandibles, palpi, legs, and antennae black with a light-red tint; males with very large metatrochanters, equal to or greater than 0.75× the length of the metafemora (Fig. 8*c*); neck constriction smooth; sides of pronotum with wrinkles laterad (extending from anterior margin to posterior margin (Fig. 7*b*); pronotal basal fovea wrinkled, with three or four medium-sized punctures that are usually obliterated by the wrinkles (Fig. 7*b*). . . . . *Diplous californicus* (Motschulsky)
   Mandibles, palpi, legs, and antennae black with a heavy red tint; males with smaller metatrochanters, less than 0.70× the length of the metafemora (Fig. 8*c*); neck constriction sparsely covered with small punctures dorsomedially; sides of pronotum with wrinkles posterolaterad only (extending from the middle of the lateral margins to the posterior margin (Fig. 7*a*,*c*); pronotal basal fovea wrinkled, without three or four medium-sized punctures (Fig. 7*a*,*c*) 3
3. Elytra subparallel to ovoid (Fig. 8*a*); elytra shiny (i.e. elytral microsculpture consisting of shallowly impressed isodiametric meshes (Fig. 8*b*); aedeagus with rounded apex, with right side incurved (Fig. 9*a*); aedeagal apical copulatory piece weakly sclerotised, somewhat twisted (Fig. 9*b*); bursal sclerite in females flat, not domed (Fig. 9*c*) . . . . . *Diplous filicornis* (Casey)
   Elytra parallel-sided (Fig. 8*a*); elytra dull (i.e. elytral microsculpture consisting of deeply impressed isodiametric meshes (Fig. 8*b*); aedeagus with square apex (Fig. 9*a*); aedeagal apical copulatory piece strongly sclerotised, spear-like (Fig. 9*b*); bursal sclerite in females domed (Fig. 9*c*) . . . . . *Diplous aterrimus* Dejean

Future research

Obtaining a better understanding of the species relationships of *Diplous* will require a more robust phylogeny based on additional gene regions and additional ingroup and outgroup taxa and specimens. Characters from different character systems should be a priority (e.g. characters of larval and pupal morphology). Only two species of *Diplous* have their larvae described and none have described pupae.

Acknowledgments

This project was supported by a Graduate Assistantship from the California Academy of Sciences. To the Entomology

Department staff at California Academy of Sciences, the first author is grateful for accommodating me as a graduate student and for providing a great research atmosphere. Thanks are also due to lenders of museum specimens (Liang Hongbin for specimens from IOZB and Stuart Hine for specimens from BMNH), and the collectors who obtained fresh specimens on my behalf (Robert Nelson for specimens from Maine and Tracy Mastranicola for specimens from Washington). We would also like to thank Greg Spicer, John Hafernik, Corrie Saux, and Alexander Zamotajlov for their help on technical and theoretical issues, as well as Jason Bond, Petra Sierwald, and anonymous reviewers for providing very helpful suggestions on the final versions of the manuscript.

References

Ball, G. E. (1972). Classification of the species of the *Harpalus* subgenus *Glanodes* Casey (Carabidae, Coleoptera). *Coleopterists Bulletin* **26**, 179–204.

Ball, G. E., and Bousquet, Y. (2001). Family 6. Carabidae. In 'American Beetles: Archostemata, Myxophaga, Adephaga, Polyphaga: Staphyliniformia'. (Eds R. H. Arnett and M. C. Thomas.) pp. 32–132. (CRC Press: Boca Raton, FL, USA.)

Bates, H. W. (1873). On the Geodephagous Coleoptera of Japan. *Transactions of the Entomological Society of London* **2**, 294–295.

Brower, A. V. Z. (1994). Rapid morphological radiation and convergence among races of the butterfly *Heliconius erato* inferred from patterns of mitochondrial DNA evolution. *Proceedings of the National Academy of Sciences of the United States of America* **91**, 6491–6495.

Chaudoir, M. (1871). Le Groupe des Pogonides. *Annales de la Société Entomologique de Belgique* **24**, 49–51.

Casey, T. L. (1918). Memoirs on the Coleoptera Vol. 8. pp. 1–427. (The New Era Printing Company: Lancaster, PA, USA.)

Darlington, P. J. (1938). The American Patrobini (Coleoptera: Carabidae). *Entomologica Americana* **18**, 135–183.

Demboski, J. R., and Cook, J. A. (2001). Phylogeography of the dusky shrew, *Sorex monticolus* (Insectivora, Soricidae): insight into deep and shallow history in northwestern North America. *Molecular Ecology* **10**, 1227–1240. doi:10.1046/j.1365-294X.2001.01260.x

Dejean, P.M.F.A (1828). Spécies général des Coléoptères de la collection de M. le Comte Dejean, Vol. 3. pp. 32–33. (Mequignon-Marvis pere et fils: Paris, France.)

Erwin, T. L. (1991). Natural history of the carabid beetles at the BIOLAT Biological Station, Rio Manu, Pakitza, Peru. *Revista Peruana de Entomologia* **33**, 1–85.

Felsenstein, J. (1981). Evolutionary trees from DNA sequences: a maximum likelihood approach. *Journal of Molecular Evolution* **17**, 368–376.

Foster, J.B. (1965). The evolution of the mammals of the Queen Charlotte Is, British Columbia. *Occasional Papers of the British Columbian Provincial Museum* **14**, 1–130.

Gebler, F. (1829). Bemerkungen über die Insekten Sibiriens, vorzüglich des Altai. In 'Reisse durch das Altai-Gebirge und die Soongorische Kirgisen-Steppe. Vol 2, Part 3'. (Ed. C. F. von Ledebour) pp. 1–228. (Reise: Berlin, Germany.)

Hansen, T. F., and Martins, E. P. (1996). Translating between microevolutionary process and macroevolutionary patterns: the correlation structure of interspecific data. *Evolution; International Journal of Organic Evolution* **50**, 1404–1407.

Hillis, D. M., and Huelsenbeck, J. P. (1992). Signal, noise, and reliability in molecular phylogenetic analyses. *The Journal of Heredity* **83**, 189–195.

Hoffman, R. L. (1963). A second species of the spider genus *Hypochilus* from eastern North America. *American Museum Novitates* **2148**, 1–8.

Huelsenbeck, J. P., and Crandall, K. A. (1997). Phylogeny estimation and hypothesis testing using maximum likelihood. *Annual Review of Ecology and Systematics* **28**, 437–466. doi:10.1146/annurev.ecolsys.28.1.437

Irwin, D. M., Kocher, T. D., and Wilson, A. C. (1991). Evolution of the cytochrome *b* gene of mammals. *Journal of Molecular Evolution* **32**, 128–144.

Kavanaugh, D. H. (1988). The insect fauna of the Pacific Northwest Coast of North America: present patterns and affinities and their origins. *Memoirs of the Entomological Society of Canada* **144**, 125–149.

Kühnelt, W. (1941). Revision der laufkäfergattungen *Patrobus* und *Diplous*. *Annalen des Naturhistorischen Museums in Wien* **51**, 151–192.

Lanave, C., Preparata, G., Saccone, C., and Serio, G. (1984). A new method for calculating evolutionary substitution rates. *Journal of Molecular Evolution* **20**, 86–93.

LeConte, J. L. (1869). List of coleoptera collected in Vancouver's I. by Henry and Joseph Matthews, with descriptions of some new species. *The Annals and Magazine of Natural History (ser. 4)* **4**, 369–385.

Lindroth, C. H. (1961). The ground-beetles (Carabidae, excl. Cicindelinae) of Canada and Alaska. Part 2. *Opuscula Entomologica Supplementum* **20**, 1–200.

Lindroth, C. H. (1975). Designation of holotypes and lectotypes among ground beetles (Coleoptera, Carabidae) described by Thomas L. Casey. *Coleopterists Bulletin* **29**, 109–147.

Maddison, D. R., Baker, M. D., and Ober, K. A. (1999). Phylogeny of carabid beetles as inferred from 18S ribosomal DNA (Coleoptera: Carabidae). *Systematic Entomology* **24**, 103–138. doi:10.1046/j.1365-3113.1999.00088.x

Maddison, W. P., and Maddison, D. R. (2000). 'MacClade, version 4.0.' (Sinauer: Sunderland, MA, USA.)

Motschulsky, V. (1844). Insectes de la Siberie rapports d'un voyage fait en 1839 et 1840. *Mémoirs de l'Academie Impériale des Sciences de St Petersbourg* **15**, 1–274.

Motschulsky, V. (1850). 'Die Kaefer Russlands. I. Insecta Carabica.' (Gautier: Moscow, Russia.)

Motschulsky, V. (1859). Coléoptères nouveaux de la Californie. *Bulletin de la Société Impériale des Naturalistes de Moscou* **32**, 122–185.

Notman, H. (1919). Records and new species of Carabidae. *Journal of the New York Entomological Society* **27**, 225–237.

Quek, S.-P., Davies, S. J., Itino, T., and Pierce, N. E. (2004). Codiversification in an ant-plant mutualism: stem texture and the evolution of host use in *Crematogaster* (Formicidae: Myrmicinae) inhabitants of *Macaranga* (Euphorbiaceae). *Evolution; International Journal of Organic Evolution* **58**, 554–570.

Randall, J. W. (1838). Descriptions of new species of coleopterous insects inhabiting the state of Maine. *Boston Journal of Natural History* **2**, 1–33.

Reichardt, H. (1977). A synopsis of the genera of Neotropical Carabidae (Insecta: Coleoptera). *Quaestiones Entomologicae* **13**, 346–493.

Rodríguez, F., Oliver, J. L., Marin, A., and Medina, J. R. (1990). The general stochastic model of nucleotide substitutions. *Journal of Theoretical Biology* **142**, 485–501.

Shelley, R. M. (1993). Revision of the milliped genus *Scytonotus* Koch (Polydesmida: Polydesmidae). *Brimleyana* **19**, 1–60.

Shimodaira, H., and Hasegawa, M. (1999). Multiple comparisons of log-likelihoods with applications to phylogenetic inference. *Molecular Biology and Evolution* **16**, 1114–1116.

Simon, C., Frati, F., Beckenbach, A., Crespi, B., Liu, H., and Flook, P. (1994). Evolution,weighting, and phylogenetic utility of mitochondrial gene sequences and a compilation of conserved polymerase chain reaction primers. *Annals of the Entomological Society of America* **Nov 1994**, 651–701.

Stone, K. D., Flynn, R. W., and Cook, J. A. (2002). Post-glacial colonization of northwestern North America by the forest-associated American marten (*Martes americana*, Mammalia: Carnivora: Mustelidae). *Molecular Ecology* **11**, 2049–2063. doi:10.1046/j.1365-294X.2002.01596.x

Swofford, D. L. (2002). 'PAUP*: Phylogenetic Analysis Using Parsimony (*and Other Methods). Version 4 ver 4.0b10'. (Sinauer: Sunderland, MA, USA.)

Tavaré, S. (1986). Some probabilistic and statistical problems on the analysis of DNA sequences. *Lectures on Mathematics and Statistics in the Life Sciences* **17**, 57–86.

Thiele, K. (1993). The Holy Grail of the perfect character: the cladistic treatment of morphometric data. *Cladistics* **9**, 275–304.

Watrous, L. E., and Wheeler, Q. D. (1981). The outgroup comparison method of character analysis. *Systematic Zoology* **30**, 1–11.

Wen, J. (1999). Evolution of eastern Asian and eastern North American disjunct distributions in flowering plants. *Annual Review of Ecology and Systematics* **30**, 421–455. doi:10.1146/annurev.ecolsys.30.1.421

Wiens, J. J. (2001). Character analysis in morphological phylogenetics: problems and solutions. *Systematic Biology* **50**, 689–699. doi:10.1080/106351501753328811

Wooding, S., and Ward, R. (1997). Phylogeography and Pleistocene evolution in the North American black bear. *Molecular Biology and Evolution* **14**, 1096–1105.

Zamotajlov, A. S. (1992). Notes on classification of the subfamily Patrobinae (Coleoptera, Carabidae) of the Palaearctic region with description of new taxa. *Bulletin de la Société Entomologique Suisse* **65**, 251–281.

Zamotajlov, A. S. (1996). Contribution to the knowledge of the Palaearctic species of the genus *Diplous* Motschulsky, 1850 (Coleoptera: Carabidae). *Zoosystematica Rossica* **5**, 107–129.

Zamotajlov, A. S. (2002). Inferring phylogenetic system of the carabid subfamily Patrobinae (Coleoptera, Carabidae). Meetings in memory of N.A. Cholodkovsky. (Zoological Institute of Russia: St. Petersburg, Russia.) Available online at: http://www.zin.ru/Animalia/Coleoptera/rus/patrob_2.pdf, verified 6 April 2004

Manuscript received 13 April 2004; revised and accepted 12 April 2005.

Appendix 1. Median values for morphometric ratios by species for males (characters: 1–31) and females (characters: 32–56)

n, species sample size; values rounded to the thousandth; numbers refer to characters listed in Table 2

Taxa (sample size)	Characters 1	2	3	4	5	6	7	8	9	10	11	12	13	14	15	16	17	18	19	20	21	22	23	24	25	26	27	28
Diplous aterrimus (*n* = 22♂, 16♀)	0.109	0.894	0.678	0.605	0.187	0.55	0.46	0.294	0.353	0.345	0.847	0.768	0.32	0.696	0.939	1.634	0.53	0.78	1.132	1.18	1	0.991	0.966	0.18	0.382	0.523	0.43	0.468
D. californicus (*n* = 23♂, 26♀)	0.103	0.915	0.585	0.545	0.192	0.549	0.483	0.304	0.306	0.295	0.856	0.812	0.385	0.746	0.876	1.583	0.895	0.829	1.093	1.152	1.053	1.094	0.932	0.167	0.237	0.61	0.801	0.65
D. filicornis (*n* = 11♂, 9♀)	0.112	0.883	0.635	0.601	0.204	0.544	0.479	0.292	0.351	0.367	0.87	0.8	0.338	0.709	0.937	1.557	0.605	0.789	1.079	1.174	0.962	1	0.915	0.175	0.387	0.511	0.364	0.52
D. rugicollis (*n* = 6♂, 9♀)	0.109	0.907	0.593	0.61	0.202	0.544	0.486	0.296	0.289	0.286	0.839	0.84	0.325	0.689	0.909	1.608	0.485	0.743	1.064	1.366	1	0.953	0.943	0.172	0.364	0.517	0.394	0.461
D. depressus (*n* = 2♂, 1♀)	0.123	0.864	0.638	0.652	0.193	0.572	0.499	0.314	0.4	0.424	0.866	0.767	0.309	0.661	0.96	1.617	0.395	0.774	1.15	1.237	1.01	0.951	0.955	0.145	0.282	0.545	0.545	?
D. sibiricus caligatus (*n* = 1♂, 1♀)	0.089	0.94	0.627	0.625	0.267	0.536	0.5	0.258	0.34	0.333	0.853	0.707	0.329	0.659	0.867	1.719	0.471	0.849	1.072	1.104	0.969	0.912	0.775	0.247	0.267	0.436	0.59	0.644
D. davidis (*n* = 1♂, 1♀)	0.092	0.994	0.713	0.637	0.223	0.583	0.492	0.344	0.364	0.386	0.829	0.747	0.309	0.638	0.955	1.684	0.447	0.87	1.026	1.03	0.946	1	0.677	0.241	0.244	0.529	0.705	0.624
D. sciakyi sciakyi (*n* = 1♂, 1♀)	0.09	0.986	0.672	0.697	0.197	0.573	0.5	0.301	0.319	0.331	0.827	0.727	0.29	0.702	1.012	1.752	0.389	0.862	1.068	1.124	1	0.883	0.86	0.184	0.348	0.46	0.56	0.56
Qiangopatrobus sp. (*n* = 1♂, 1♀)	0.103	0.967	0.661	0.684	0.207	0.6	0.469	0.388	0.376	0.359	0.855	0.717	0.3	0.607	1.06	1.502	0.389	0.776	1.064	1.008	0.992	0.98	0.784	0.208	0.294	0.669	0.555	0.598

Appendix 1. (continued)

Taxa (sample size)	Characters 29	30	31	32	33	34	35	36	37	38	39	40	41	42	43	44	45	46	47	48	49	50	51	52	53	54	55	56
Diplous aterrimus (*n* = 22♂, 16♀)	0.424	1.148	0.475	0.107	0.904	0.654	0.618	0.176	0.561	0.452	0.297	0.34	0.339	0.841	0.787	0.307	0.684	0.963	1.627	0.445	0.74	0.936	1	0.969	0.92	0.972	0.165	?
D. californicus (*n* = 23♂, 26♀)	0.559	1.511	0.662	0.104	0.915	0.549	0.571	0.19	0.576	0.469	0.287	0.29	0.292	0.859	0.808	0.345	0.693	0.935	1.634	0.507	0.755	0.962	1.011	1.041	1.105	0.905	0.163	0.052
D. filicornis (*n* = 11♂, 9♀)	0.461	1.341	0.476	0.107	0.932	0.603	0.613	0.195	0.558	0.471	0.288	0.345	0.357	0.855	0.8	0.322	0.692	0.932	1.645	0.504	0.762	0.964	1.011	0.975	0.94	0.926	0.163	0.057
D. rugicollis (*n* = 6♂, 9♀)	0.444	1.227	0.442	0.111	0.904	0.578	0.625	0.21	0.539	0.472	0.305	0.274	0.269	0.865	0.84	0.31	0.675	0.934	1.66	0.439	0.715	0.949	1.066	1	0.971	0.966	0.165	0.066
D. depressus (*n* = 2♂, 1♀)	0.508	1.271	0.477	0.105	0.948	0.604	0.667	0.175	0.565	0.473	0.33	0.387	0.387	0.843	0.745	0.283	0.671	0.962	1.729	0.375	0.753	1	0.949	0.956	1.011	0.907	0.061	0.051
D. sibiricus caligatus (*n* = 1♂, 1♀)	0.59	1.415	0.524	0.094	0.979	0.671	0.648	0.277	0.521	0.526	0.211	0.371	0.351	0.88	0.72	0.284	0.646	0.945	1.742	0.452	0.79	0.94	1.012	0.98	0.94	0.732	0.256	0.043
D. davidis (*n* = 1♂, 1♀)	0.584	?	?	0.095	1	0.671	0.633	0.235	0.57	0.502	0.365	0.373	0.376	0.869	0.697	0.29	0.605	1.014	1.61	0.417	0.756	0.184	0.914	4.578	1.083	0.723	0.27	0.069
D. sciakyi sciakyi (*n* = 1♂, 1♀)	0.52	1.08	0.37	0.101	0.904	0.702	0.651	0.212	0.564	0.474	0.331	0.281	0.281	0.885	0.752	0.292	0.67	0.96	1.715	0.361	0.824	0.991	0.94	0.992	0.825	0.836	0.224	0.044
Qiangopatrobus sp. (*n* = 1♂, 1♀)	0.583	1.551	0.404	0.083	1.147	0.658	0.67	0.179	0.605	0.467	0.378	0.356	0.391	0.86	0.746	0.282	0.598	1.048	1.545	0.361	0.748	1	1	0.897	0.816	0.833	0.272	0.07

Appendix 2. Morphology character state matrix (TreeBASE Acc. M2288)

Taxon	1	2	3	4	5	6	7	8	9	10	11	12	13	14	15	16	17	18	19	20	21	22	23	24	25	26	27	28	29	30	31	32	33	34	35	36	37	38	39	40	41	42	43	44	45	46	47	48	49
Diplous aterrimus	5	2	7	2	0	4	0	2	5	4	3	5	4	5	4	5	6	3	6	6	4	5	8	4	7	4	2	1	0	1	3	7	0	4	2	1	3	0	3	3	3	0	5	5	6	6	2	5	1
D. californicus	3	4	0	0	1	3	3	5	1	1	6	7	8	8	1	2	8	5	5	4	6	7	5	1	0	7	8	7	5	6	7	4	1	0	0	3	7	2	1	2	2	3	7	8	8	2	3	8	4
D. filicornis	7	1	3	1	5	2	2	1	4	6	8	6	7	7	3	1	7	4	4	5	1	6	4	3	8	2	0	2	2	4	4	6	2	2	1	4	2	3	2	4	5	2	6	7	7	0	4	7	6
D. rugicollis	6	3	1	3	4	1	4	3	0	0	2	8	5	4	2	3	5	0	1	8	4	3	6	2	6	3	1	0	1	2	2	8	0	1	3	5	1	4	4	0	0	5	8	6	5	1	5	4	0
D. depressus	8	0	4	6	2	5	6	6	8	8	7	4	2	3	6	4	2	1	7	7	5	2	7	0	3	6	3	?	3	3	5	5	3	3	7	0	5	5	5	8	7	1	2	1	4	5	7	2	3
D. sibiricus caligatus	0	5	2	4	8	0	7	0	3	3	4	0	6	2	0	7	4	6	3	2	2	1	1	8	2	0	6	6	8	5	6	1	4	7	5	8	0	8	0	6	4	7	1	2	2	3	8	6	7
D. davidis	2	8	8	5	7	7	5	7	6	7	1	3	3	1	5	6	3	8	0	1	0	6	0	7	1	5	7	5	7	?	?	2	5	6	4	7	6	7	7	7	6	6	0	3	1	7	1	3	5
D. sciakyi sciakyi	1	7	6	8	3	6	7	4	2	2	0	2	0	6	7	8	1	7	2	3	4	0	3	5	5	1	5	3	4	0	0	3	0	8	6	6	4	6	6	1	1	8	4	4	3	4	6	0	8
Qiangopatrobus sp.	4	6	5	7	6	8	1	8	7	5	5	1	1	0	8	0	0	2	1	0	3	4	2	6	4	8	4	4	6	7	1	0	6	5	8	2	8	1	8	5	8	4	3	0	0	8	0	1	2

Appendix 2. (continued)

Taxon	50	51	52	53	54	55	56	57	58	59	60	61	62	63	64	65	66	67	68	69	70	71	72	73	74	75	76	77	78	79	80	81	82	83	84	85	86	87	88	89	90	91	92	93	94	95	96	97
Diplous aterrimus	1	3	2	2	8	3	?	1	0	1	1	1	0	1	1	0	0	0	2	0	2	2	3	2	1	1	0	0	2	1	2	1	3	1	0	0	2	1	1	1	1	1	1	0	2	1	1	0
D. californicus	4	4	7	7	4	2	3	1	1	0	0	0	0	2	1	1	1	0	3	1	3	3	0	2	1	1	1	1	2	2	3	2	0	1	0	0	2	1	1	2	1	1	0	0	2	1	1	0
D. filicornis	5	5	3	3	6	1	4	1	0	1	1	2	0	1	1	0	1	0	2	1	2	2	3	1	1	0	0	0	2	1	2	1	2	1	0	0	1	1	1	2	1	1	1	1	2	0	1	0
D. rugicollis	3	7	6	4	7	3	5	1	0	2	0	1	0	1	0	0	0	1	1	1	1	1	2	2	1	0	0	0	1	0	1	0	2	1	0	0	0	1	1	1	1	1	1	0	1	1	1	0
D. depressus	7	2	1	5	5	0	2	1	0	2	3	2	1	1	0	0	0	1	1	0	1	1	2	2	1	0	0	0	0	0	1	0	0	1	0	0	1	1	1	0	0	1	0	3	2	1	1	0
D. sibiricus caligatus	2	6	4	3	1	5	0	0	0	3	2	1	0	0	0	0	0	1	1	0	3	2	1	2	0	0	0	0	1	0	1	0	0	0	0	2	2	0	0	0	0	1	0	2	2	0	0	0
D. davidis	0	0	8	6	0	6	6	0	0	2	2	2	1	0	2	0	0	1	0	0	1	0	2	0	0	1	0	0	0	0	0	0	0	0	0	2	2	0	0	0	0	1	0	0	0	0	0	1
D. sciakyi sciakyi	6	1	5	1	3	4	1	1	0	2	1	2	0	0	0	0	0	0	1	0	2	0	1	2	0	1	0	0	0	0	0	0	1	1	1	1	2	0	1	0	0	1	0	0	0	0	0	1
Qiangopatrobus sp.	7	3	0	0	2	7	7	1	2	2	1	1	0	0	0	0	0	0	0	0	0	0	0	0	0	0	0	0	0	0	0	0	0	0	0	0	0	0	0	0	0	0	0	0	0	0	0	0